La gravimétrie spatiale

réalisations et perspectives

Richard Biancale CNES/GRGS

Journées scientifiques GRAM 2016, APC Paris, 2-3 juin 2016

Satellite missions for gravity field determination

1961 – 2000
Earth tracking
100 m – 1 cm

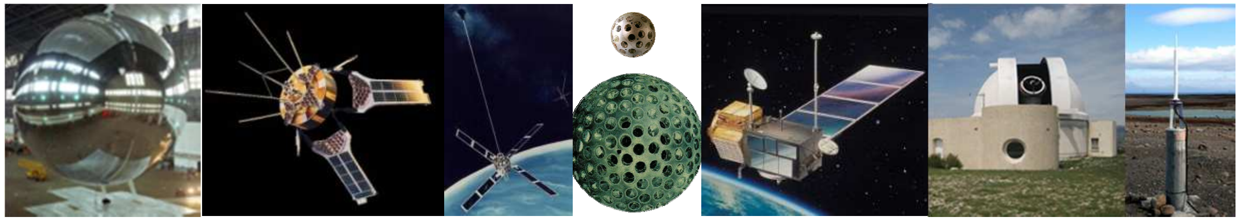

camera
TRANSIT
SLR
PRARE
DORIS

2000 – 2010
High-low tracking
1 cm

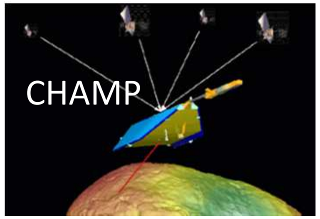

GPS + SLR + accelerometer

2002 – …
Low-low tracking
1 µm

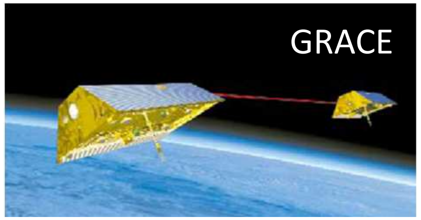

GPS + SLR + KBR + accelerometer

2009 – 2013
In situ measurement
3 mE (10^{-9} s^{-1})

GPS + SLR + gradiometer

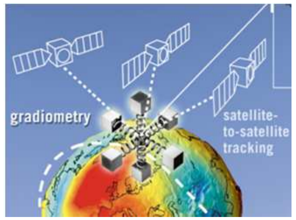

2017 – …
Low-low tracking
50 nm

GPS + SLR + KBR + LRI + accelerometer

GRACE decay

Gravity Recovery And Climate Experiment

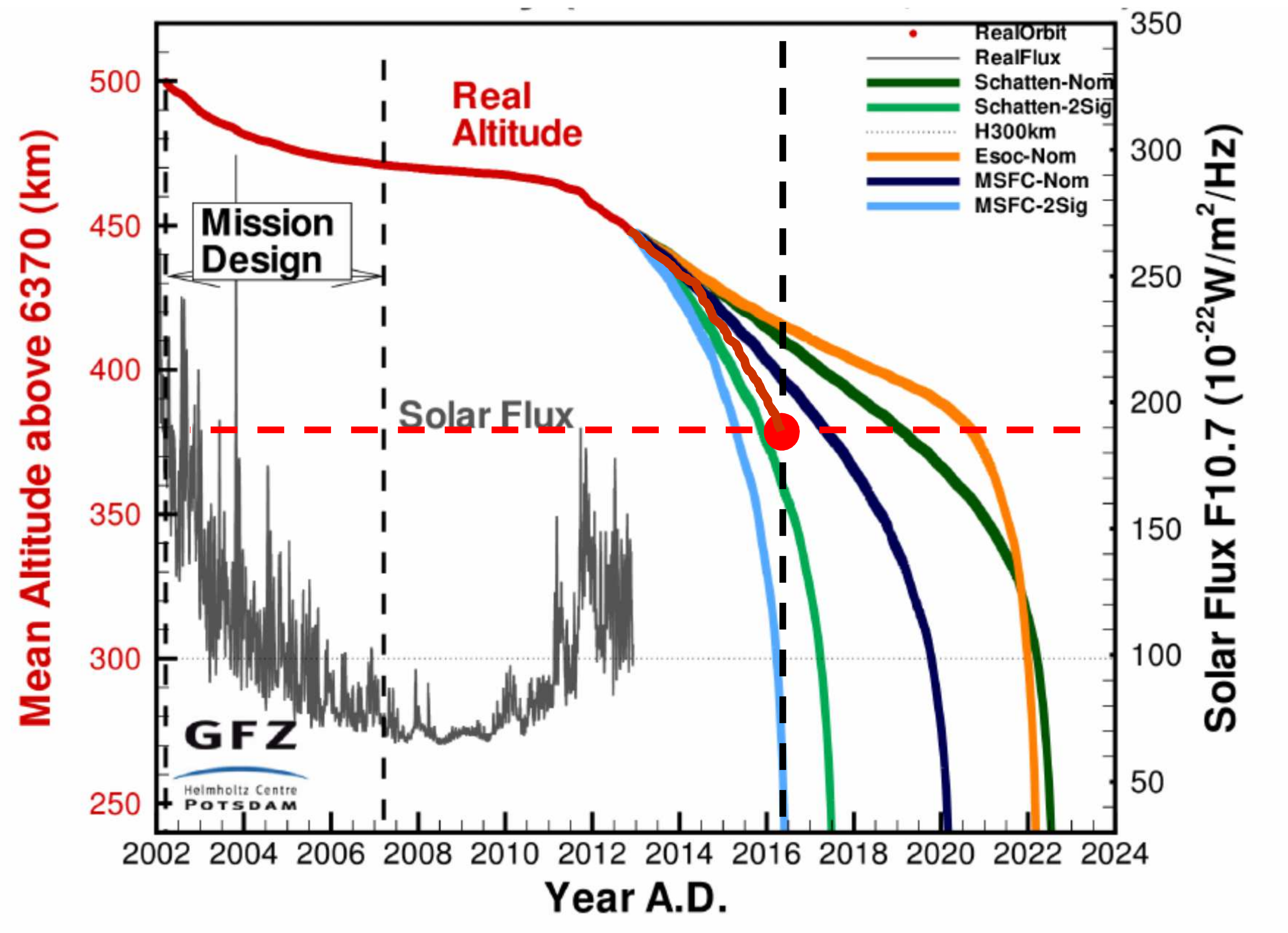

GOCE

Gravity field and steady-state Ocean Circulation Explorer

17 March 2009 – 11 November 2013

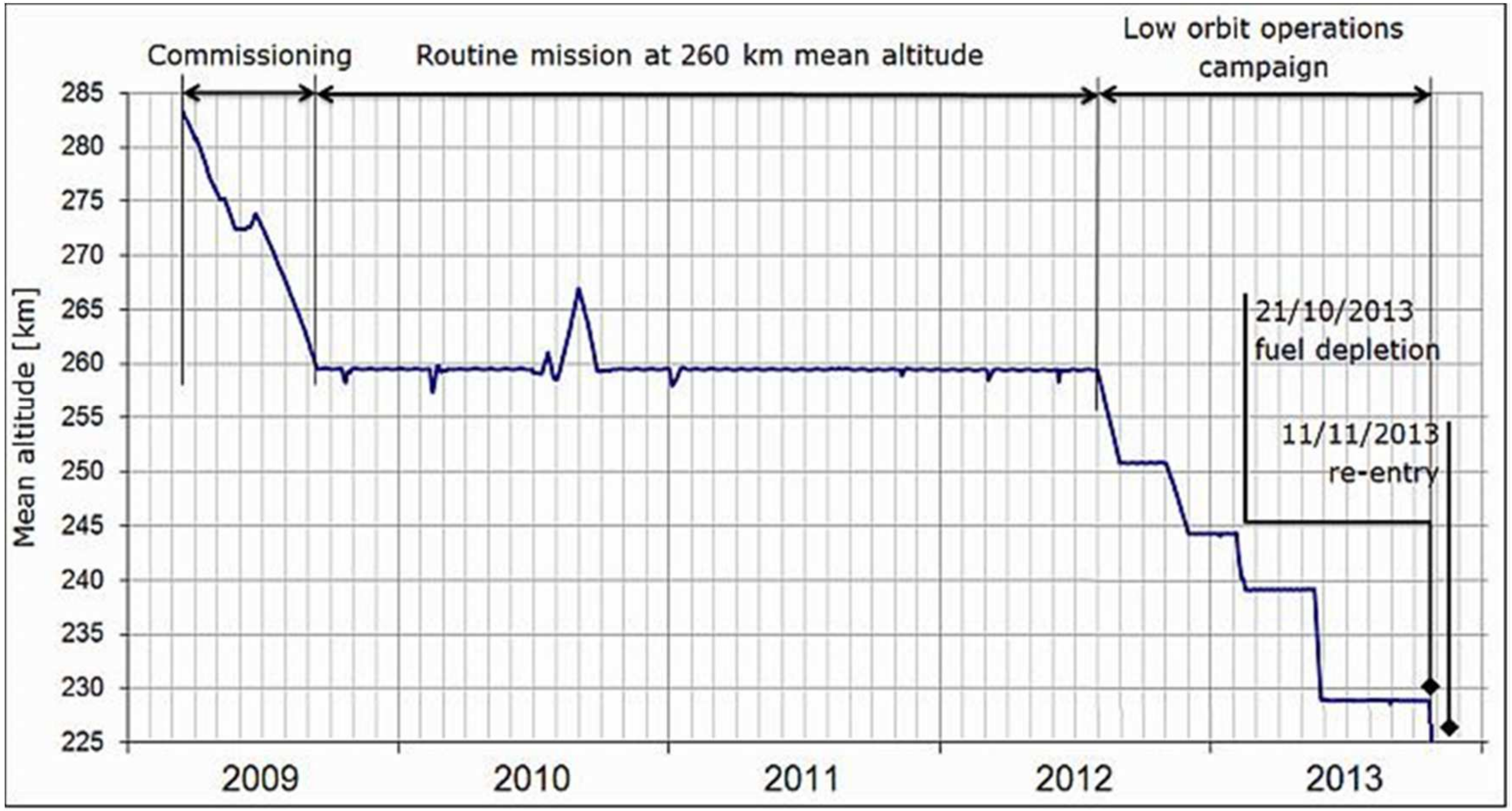

Spatio-temporal level of gravity field measurements

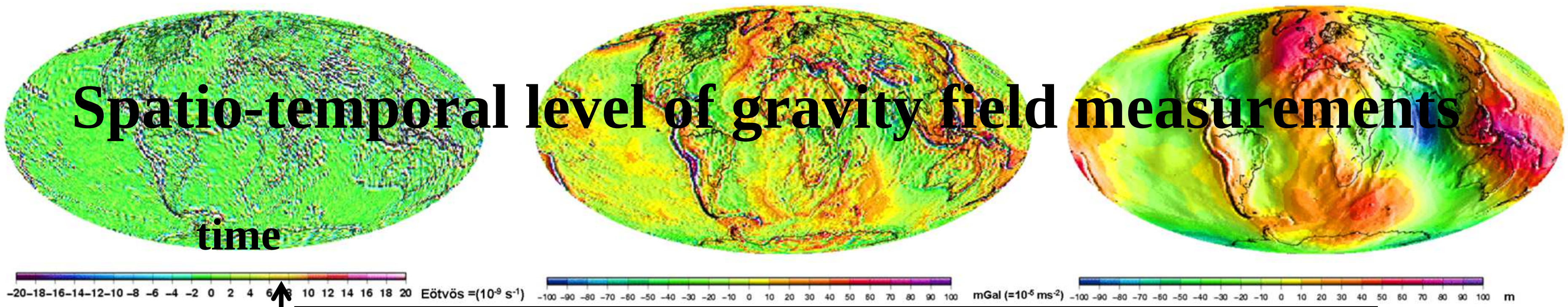

time derivative

> sensitivity

t

$$\bar{r} = \iint \ddot{\bar{r}}\, dt$$

d /dt

$$\Delta U_{AB} = \frac{1}{2}\left|\Delta \dot{r}_{AB}\right|^2 - \ldots$$

d^2 /dt^2

$(R/r)^{l+3}$

$$\begin{pmatrix} \frac{\partial^2 U}{\partial x^2}, \frac{\partial^2 U}{\partial x \partial y}, \frac{\partial^2 U}{\partial x \partial z} \\ \frac{\partial^2 U}{\partial y \partial x}, \frac{\partial^2 U}{\partial y^2}, \frac{\partial^2 U}{\partial y \partial z} \\ \frac{\partial^2 U}{\partial z \partial x}, \frac{\partial^2 U}{\partial z \partial y}, \frac{\partial^2 U}{\partial z^2} \end{pmatrix}$$

Radial gradient :

$\partial^2 U/\partial r^2 = R\gamma \sum (l+1)(l+2)\, H_l$

$(R/r)^{l+2}$

$$\ddot{\bar{r}} = \left(\frac{\partial U}{\partial x}, \frac{\partial U}{\partial y}, \frac{\partial U}{\partial z} \right)$$

Gravity anomaly :

$\Delta g = -\,\partial T/\partial r - 2T / r$

$= \gamma \sum (l-1)\, H_l^*$

$(R/r)^{l+1}$

$$U = \int \ddot{\bar{r}}\, d\bar{s}$$

$$U_{géoïde} = C^{te}$$

Geoid height **:**

$N = T / \gamma = (U-V) / \gamma$

$= R \sum H_l^*$

Laplace's equation :

$\partial^2 U/\partial x^2 + \partial^2 U/\partial y^2 + \partial^2 U/\partial z^2 = 0$

$\partial^2 /\partial s^2$ $\partial /\partial s$ *s* **space**

space differentiation

> resolution

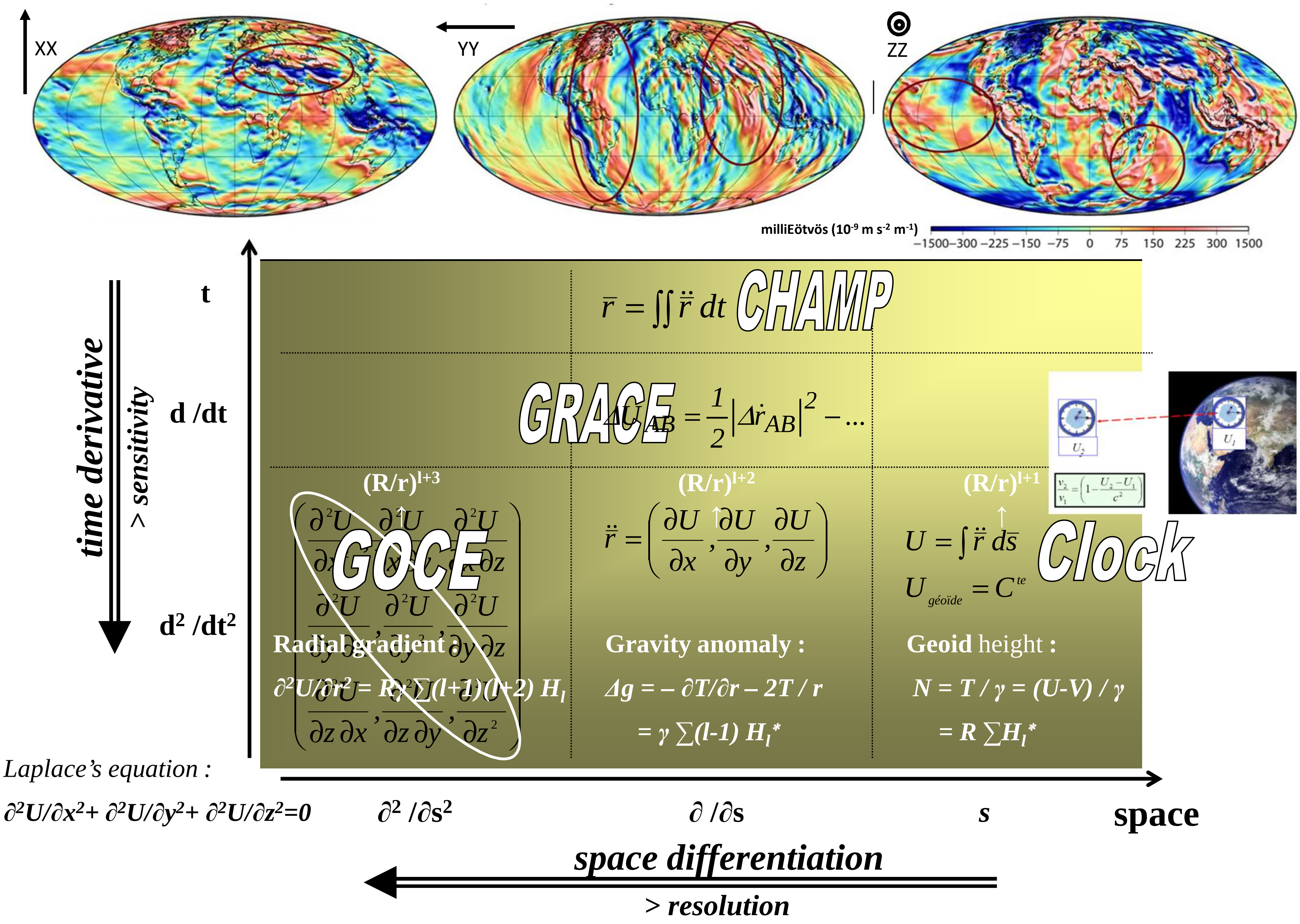
XX
YY
ZZ
milliEötvös (10-9 m s-2 m-1)
−1500 −300 −225 −150 −75 0 75 150 225 300 1500
t
d /dt
d2 /dt2
time derivative
> sensitivity
CHAMP
GRACE
GOCE
Clock
(R/r)l+3
(R/r)l+2
(R/r)l+1
Radial gradient :
Gravity anomaly :
Geoid height :
Δg = – ∂T/∂r – 2T / r
= γ ∑(l-1) Hl*
N = T / γ = (U-V) / γ
= R ∑Hl*
Laplace's equation :
∂2U/∂x2+ ∂2U/∂y2+ ∂2U/∂z2=0
∂2 /∂s2
∂ /∂s
s
space
space differentiation
> resolution

Modelling in spherical harmonic functions

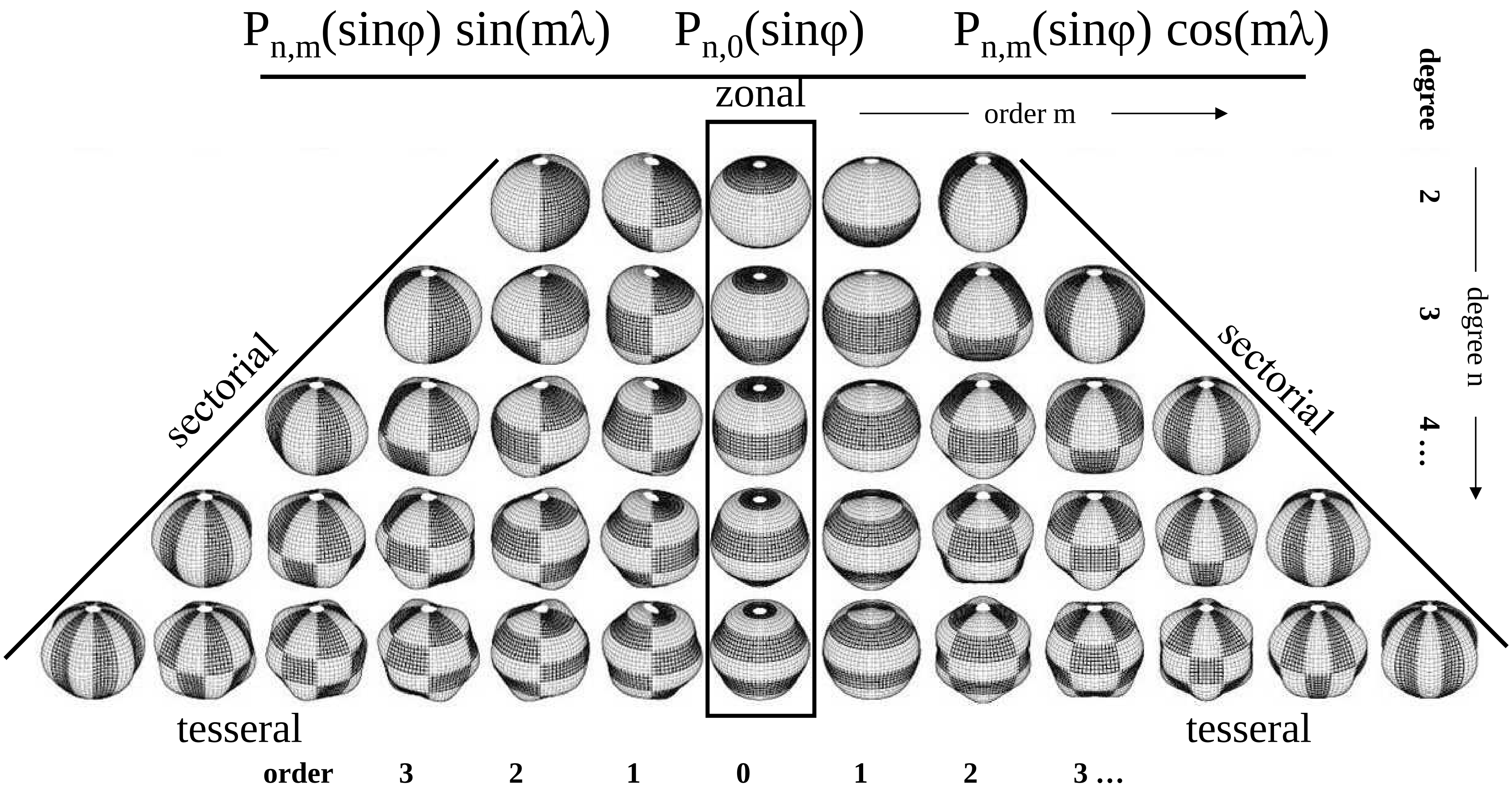

$$U = \frac{GM}{a_e}\sum_{n=0}^{\infty}\left(\frac{a_e}{r}\right)^{n+1}\sum_{m=0}^{n}P_{n,m}(\sin\varphi)\left(C_{n,m}\cos m\lambda + S_{n,m}\sin m\lambda\right)$$

Error spectra of global gravity field models

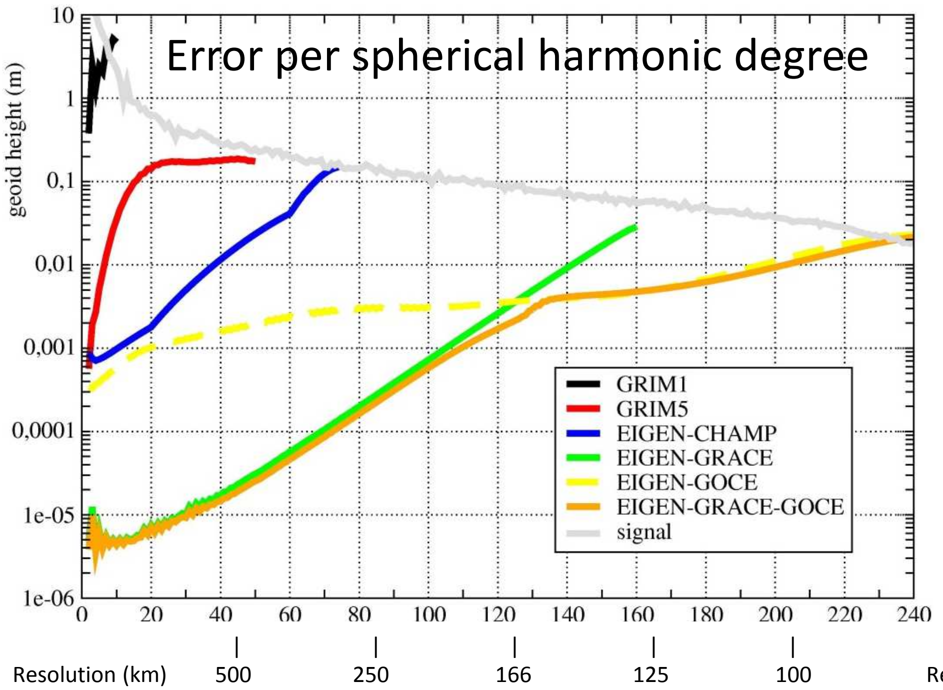

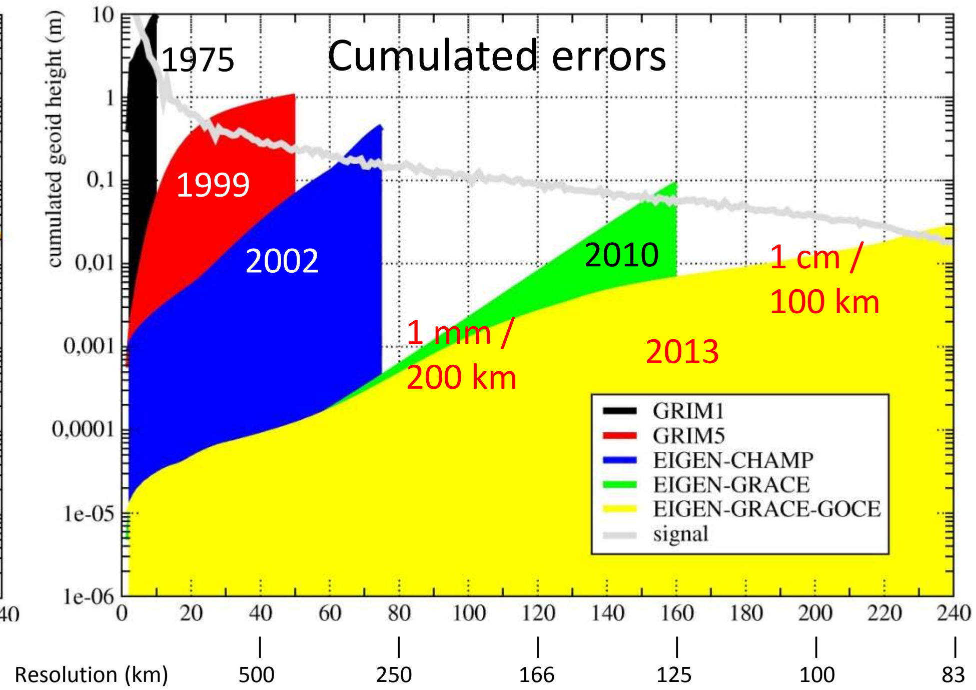

EIGEN6-C4 (2014)

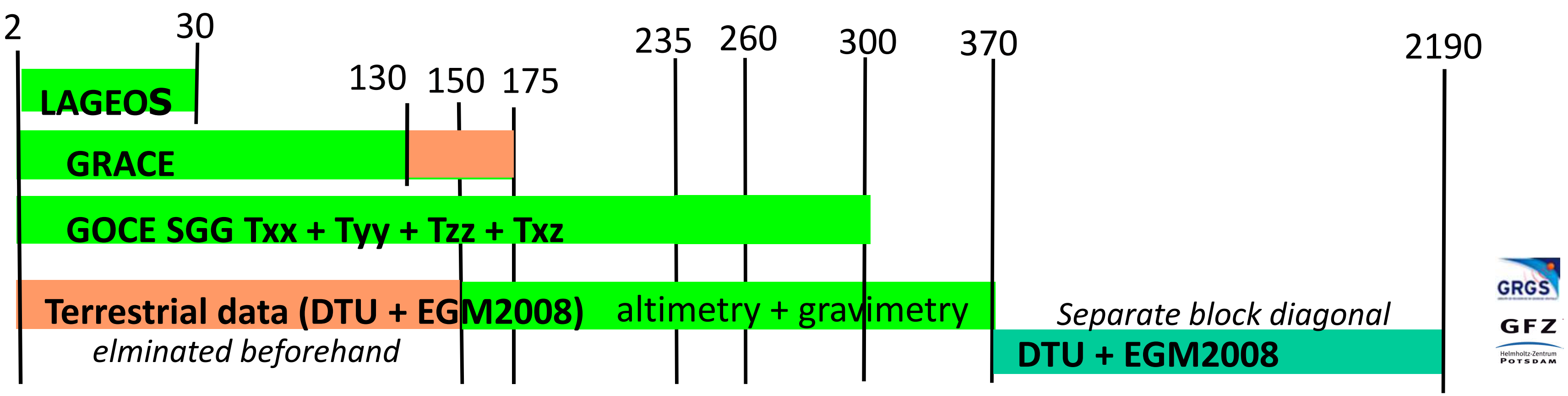

Modelling the Earth gravity field

Potential of gravitation:

±1000 m² s⁻² Clock

$$U = \frac{GM}{a_e}\sum_{l=0}^{L}\left(\frac{a_e}{r}\right)^{l+1}\sum_{m=0}^{l}\overline{P}_{l,m}(\sin\varphi)\left(\overline{C}_{l,m}\cos m\lambda + \overline{S}_{l,m}\sin m\lambda\right)$$

$$U_0 = 62\,494\,812.4\ m^2 s^{-2}$$

Orbital perturbation:

±1000 m GRACE

(10 km /C_{20})

$$\ddot{\overline{x}} = \frac{\partial U}{\partial \overline{x}} \quad \textit{numerical or analytical integration (Lagrange's equation)}$$

$$\frac{\partial U}{\partial r} = -\frac{GM}{a_e^2}\sum_{l=0}^{L}(l+1)\left(\frac{a_e}{r}\right)^{l+2}\sum_{m=0}^{l}\overline{P}_{l,m}(\sin\varphi)\left(\overline{C}_{l,m}\cos m\lambda + \overline{S}_{l,m}\sin m\lambda\right)$$

Geoid height:

±100 m Altimeter

$$N = \frac{T}{\gamma}\ , \quad T = U - V,\quad V: \textit{ellipsoid potential}$$

$$N = a_e\sum_{l=0}^{L}\sum_{m=0}^{n}\overline{P}_{l,m}(\sin\varphi)\left(\overline{C}^*_{l,m}\cos m\lambda + \overline{S}^*_{l,m}\sin m\lambda\right)$$

Gravity anomaly:

±500 mGal Gravimeter

(mGal=10^{-5} m s^{-2})

$$\Delta g = \frac{\partial T}{\partial r} + 2\frac{T}{r}$$

$$\Delta g = \frac{GM}{a_e^2}\sum_{l=0}^{L}(l-1)\sum_{m=0}^{n}\overline{P}_{l,m}(\sin\varphi)\left(\overline{C}^*_{l,m}\cos m\lambda + \overline{S}^*_{l,m}\sin m\lambda\right)$$

Vertical deflection:

±50 “ Tiltmeter

$$\xi = -\frac{1}{r\gamma}\frac{\partial T}{\partial\theta};\quad \eta = -\frac{1}{r\gamma\cos\varphi}\frac{\partial T}{\partial\lambda}$$

Gravity gradient:

±50 Eötvös GOCE

(Eötvös=10^{-9} s^{-2})

$$\frac{\partial^2 U}{\partial r^2} = \frac{GM}{a_e^3}\sum_{l=0}^{L}(l+1)(l+2)\left(\frac{a_e}{r}\right)^{l+3}\sum_{m=0}^{l}\overline{P}_{l,m}(\sin\varphi)\left(\overline{C}_{l,m}\cos m\lambda + \overline{S}_{l,m}\sin m\lambda\right)$$

The GRACE signal and its transformation

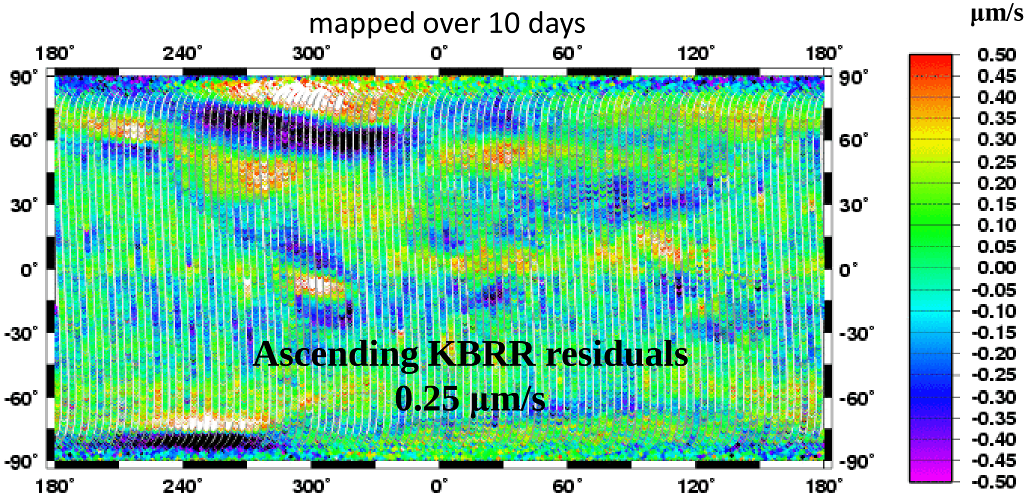

Biased range data derived

$$\rightarrow \quad \Delta U_{AB} = \frac{1}{2}\left|\Delta v_{AB}\right|^2 - \ldots$$

according to the energy integral approach

× R

$$\Delta h^{water} = \frac{g}{4\pi G R \rho_w} \sum_{l=2}^{80} \frac{2l+1}{1+k_l'} \Delta h_l^{geoid}$$

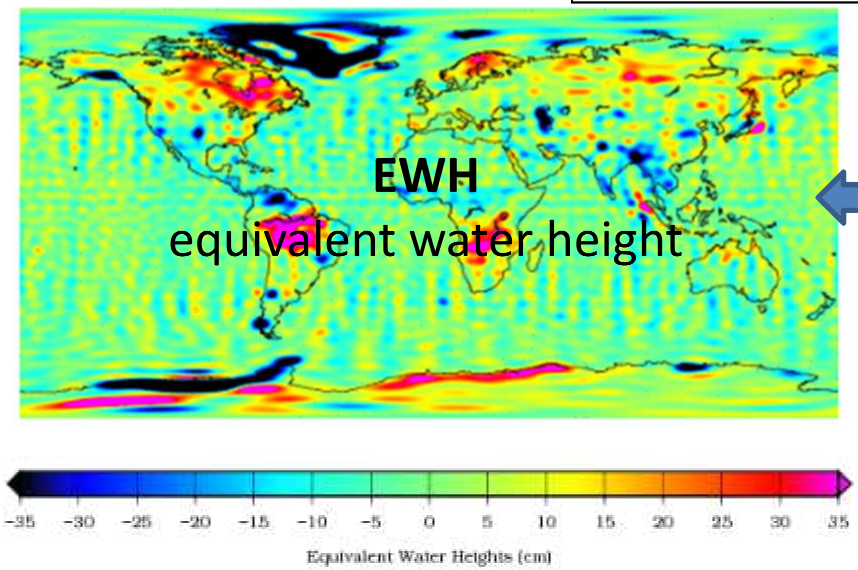

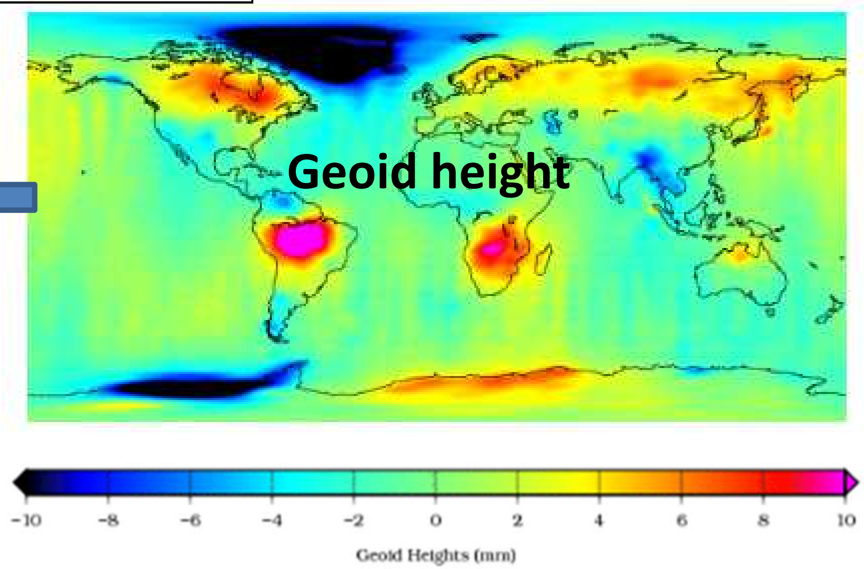

GRACE inversion technique

- **Inversion technique used for RL03 : truncated Singular Value Decomposition (SVD)**

  - It is more efficient to solve well chosen linear combinations of coefficients (by truncated SVD) than to solve indistinctly the coefficients (by Cholesky decomposition).

  - Demonstration with a normal matrix up to d/o 80:

    1) Solving for the first 2601 components of the canonical basis (i.e. spherical harmonic coefficients up to degree/order 50)

    2) Solving for the first 2601 components of the basis made by the eigenvectors of the normal matrix

- **The 2 step approach**

  - Since SVD does not solve sectorial coefficients due to a lack of information, we need to introduce decent a-priori sectorial coefficients before using SVD

  - So we tried to establish a 2-step inversion in RL03-v2

    - First step: Cholesky inversion with constraints to obtain good sectorial coefficients

    - Second step: Truncated SVD inversion starting with the first step solution

1) Cholesky decomposition

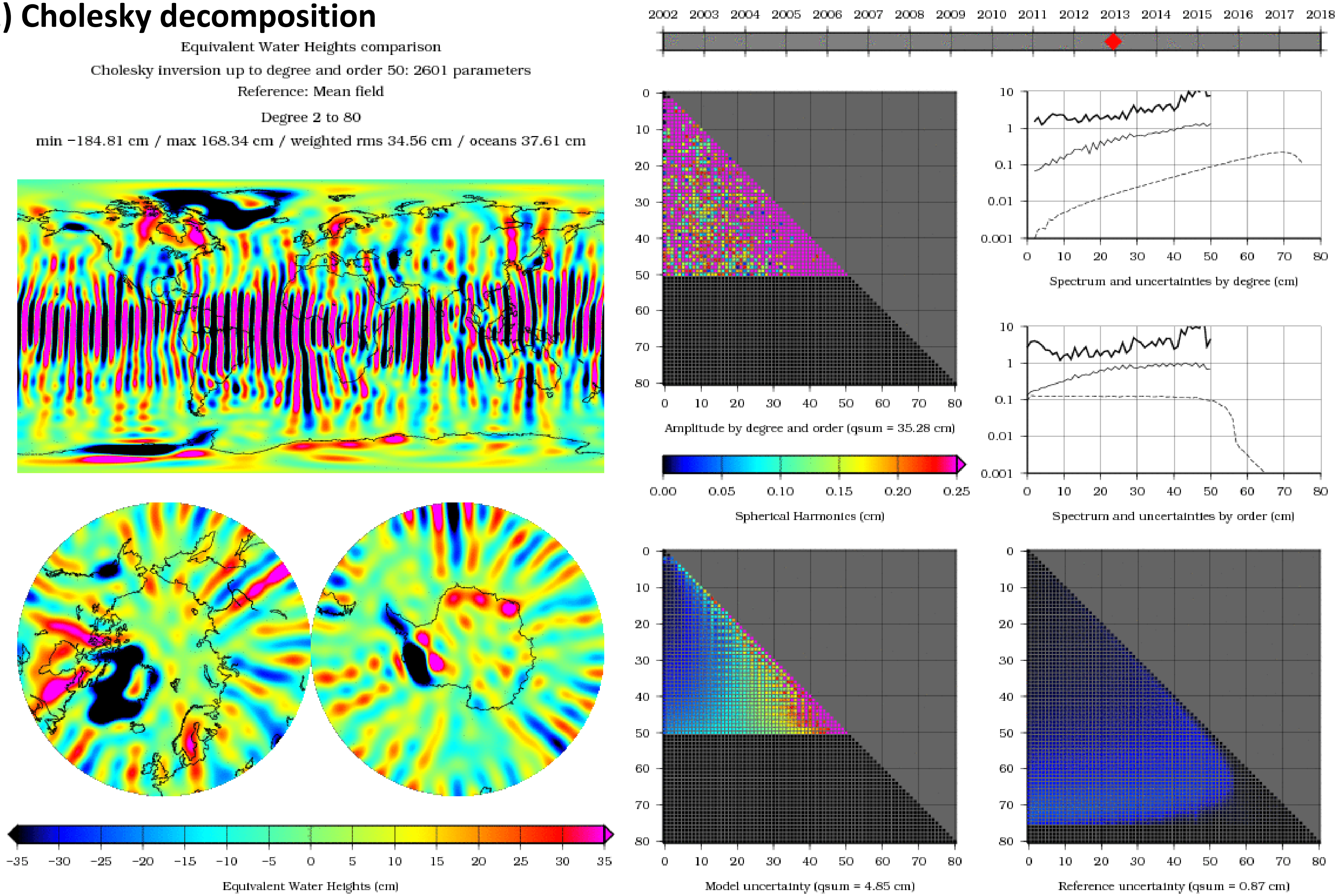

2) Truncated SVD

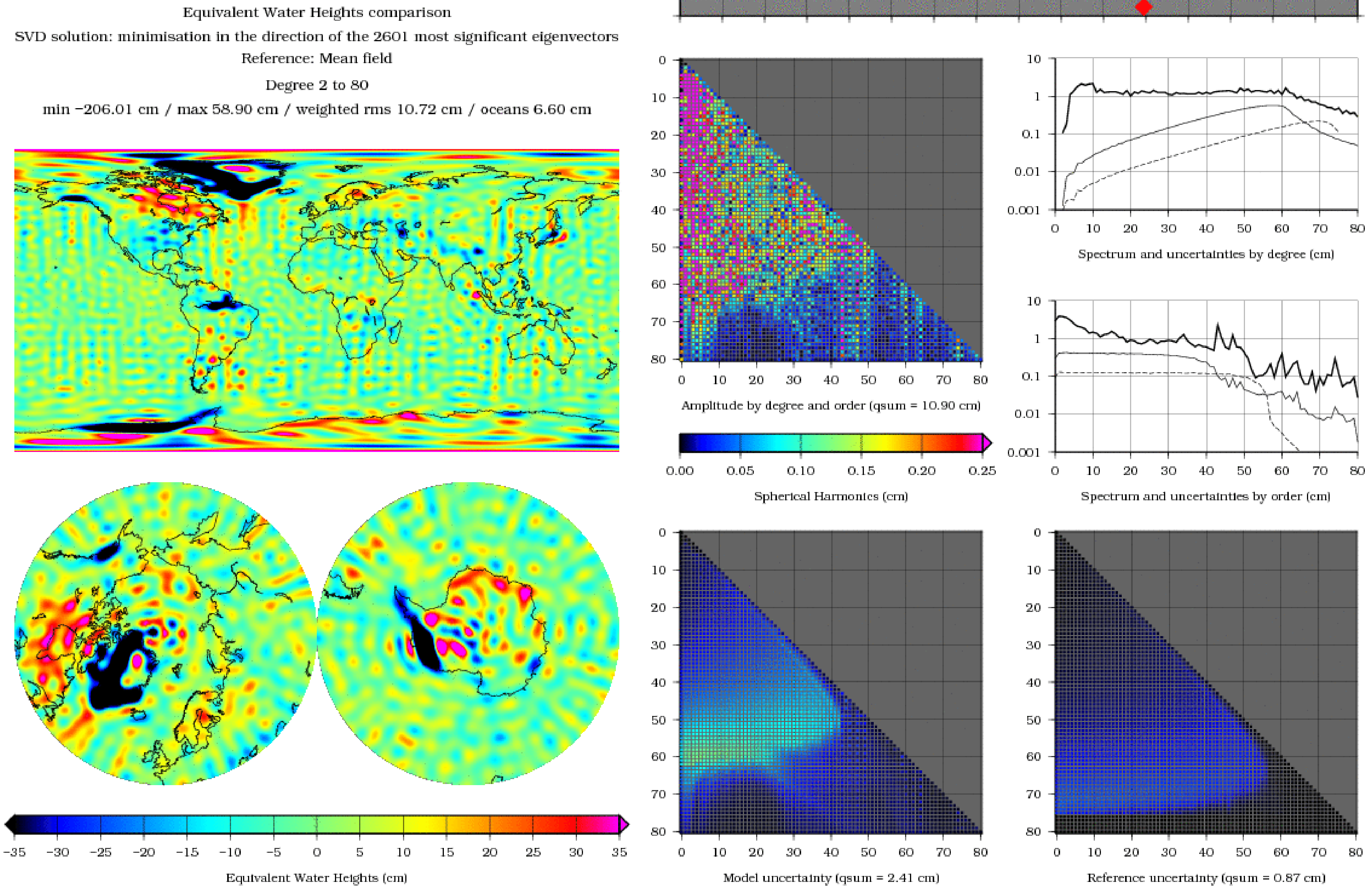

3) 2-step approach: RL03-v2

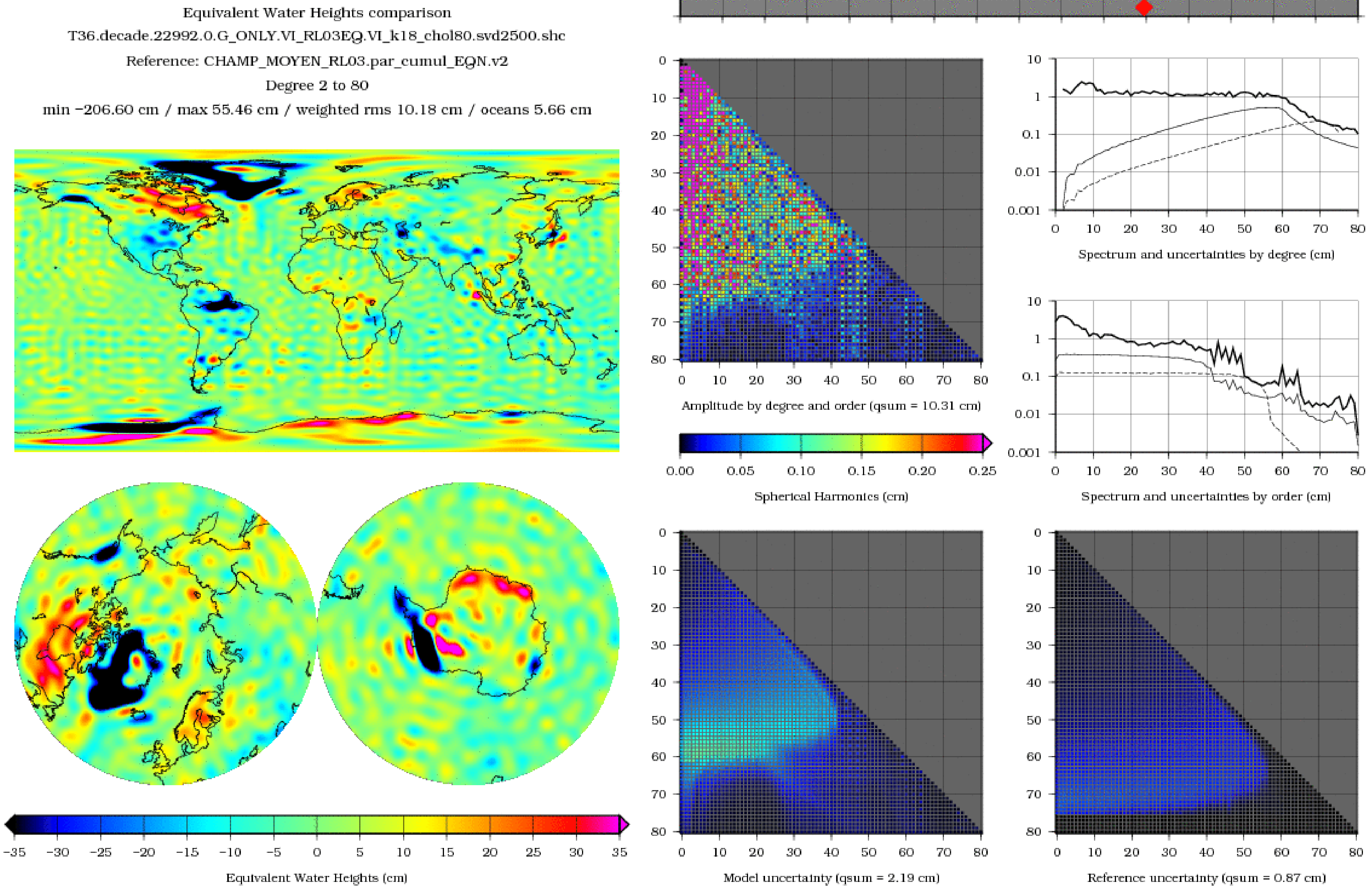

Error spectra of global time variable gravity field models

When converting volume potential into surface potential → surface mass displacement in EWH

*Signal and error per spherical harmonic degree in **equivalent water height** (EWH)*

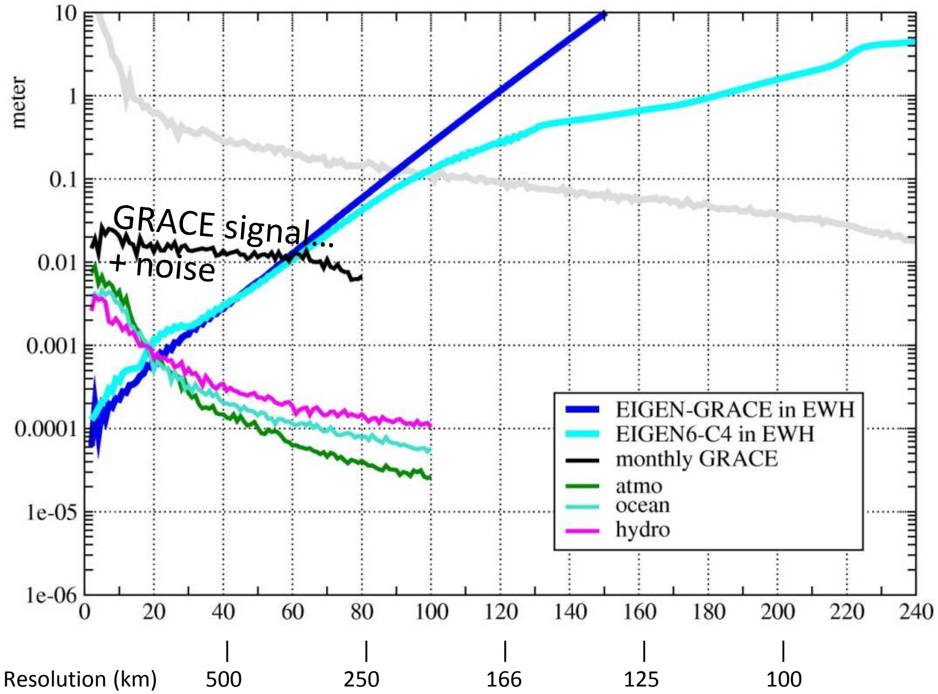

$$\Delta h^{water} = \frac{g}{4\pi G R \rho_w} \sum_{l=2}^{50} \frac{2l+1}{1+k_l'} \Delta h_l^{geoid}$$

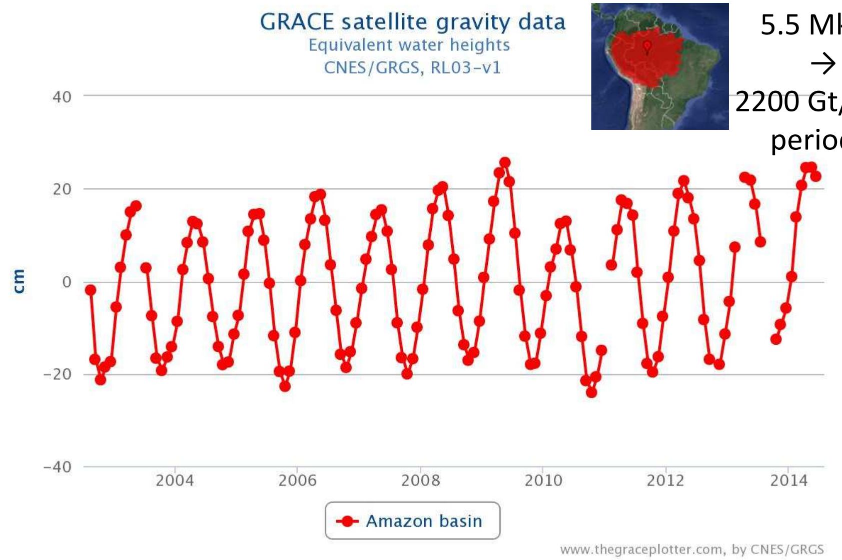

5.5 Mkm^2
→
2200 Gt/sem.
periodic

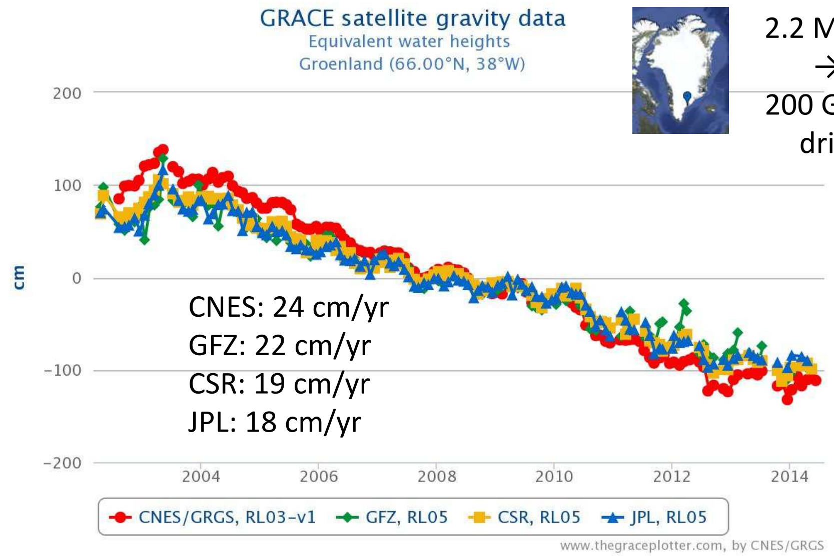

2.2 Mkm^2
→
200 Gt/yr
drift

GRGS

The problem of a posteriori filtering

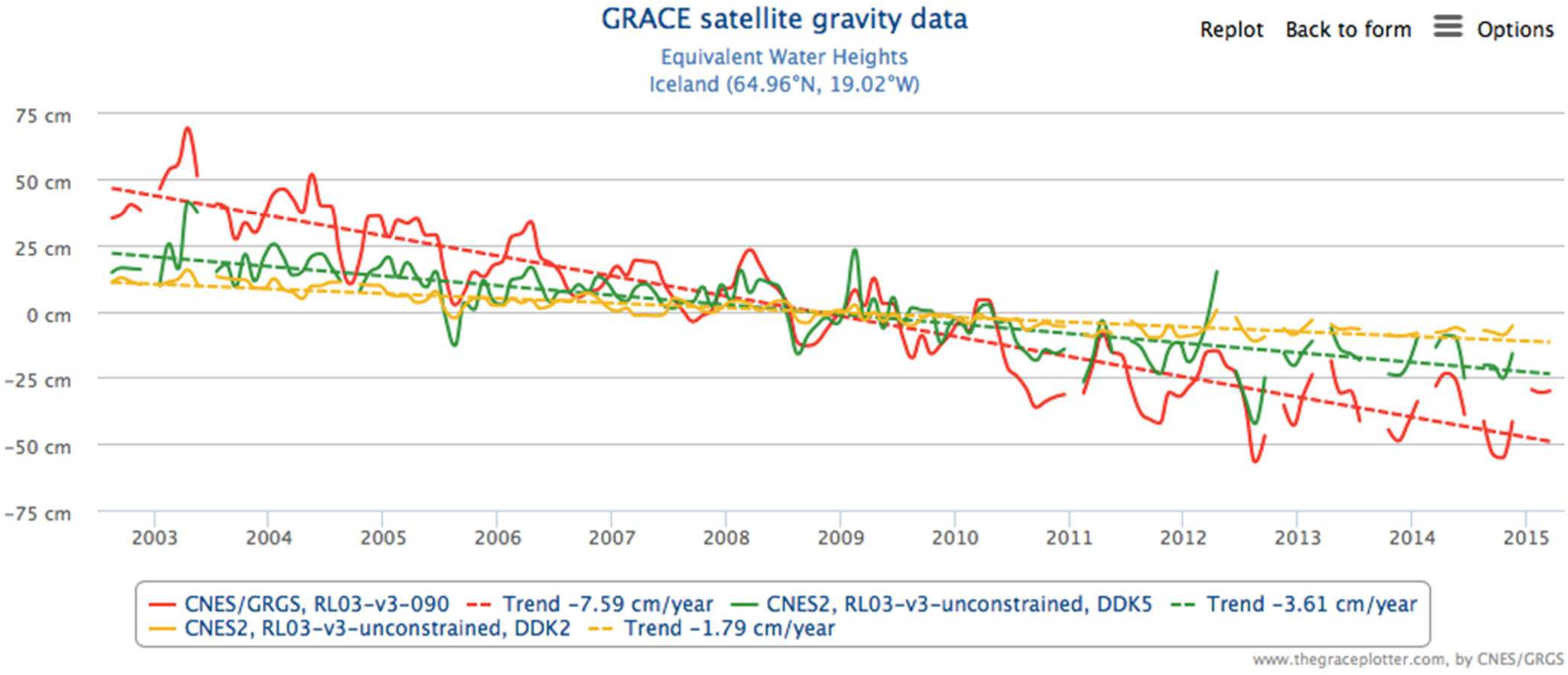

GRACE mean model

❖ **Mean Models generated from time series**

- Fitting each series of monthly coefficients by a set of 6 parameters
- Used for operational computation (i.e. altimetric orbit processing) or TRF processing (i.e. ITRF2014)
- In order to better match with GRACE observations, gravity field models have become more complex. They contain now :
  - Yearly bias and slope : piecewise linear function except in case of …
  - Jumps caused by big earthquakes (3 so far : Sumatra, Concepcion and Tohoku)
  - Annual and semi-annual sine/cosine functions (with continuity constraints at hinge epochs)

… it means 600 000 coefficients for a 80x80 s. h. model

Mean model

“bias and slope” vs. “piece-wise-linear” modelling

“bias and slope”
EIGEN-GRGS.RL02bis.MEAN-FIELD

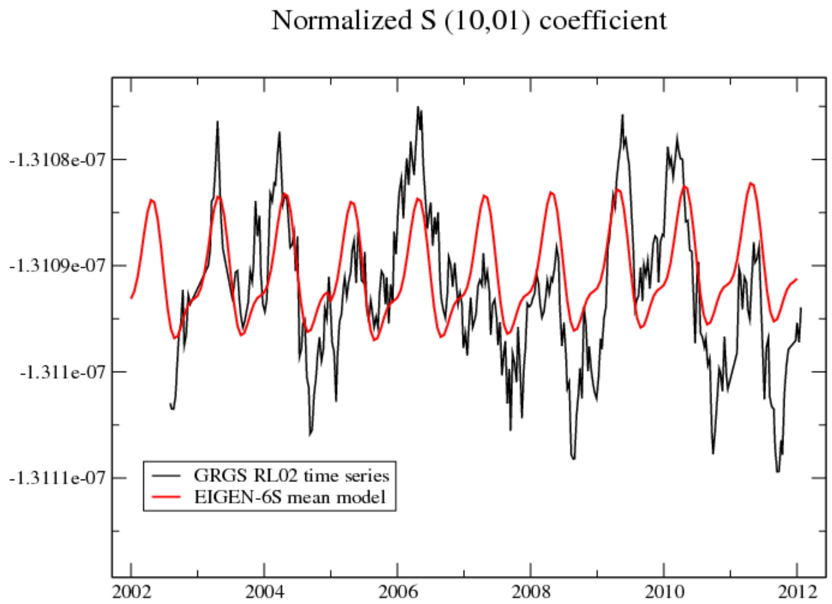

“piece-wise-linear”
EIGEN-GRGS.RL03.MEAN-FIELD

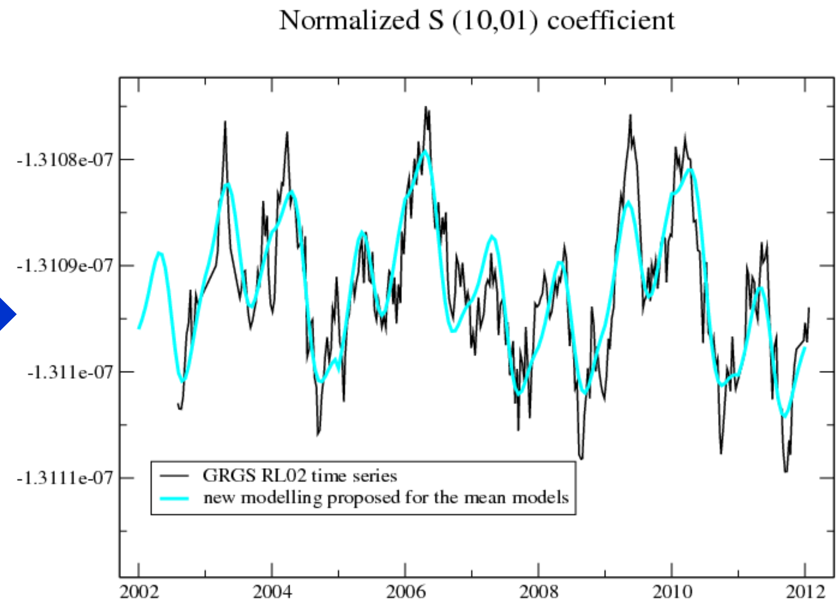

Example of format

```
G_BIAS    2    0 -.484165479521E-03 0.000000000000E+00 0.1392E-10 0.0000E+00 19500101.0000 19850109.1751
GDRIFT    2    0 0.104634158251E-11 0.000000000000E+00 0.5603E-12 0.0000E+00 19500101.0000 19850109.1751
G_BIAS    2    0 -.484165356094E-03 0.000000000000E+00 0.7295E-11 0.0000E+00 19900101.0000 19910101.0000
GDRIFT    2    0 0.162048658823E-10 0.000000000000E+00 0.1449E-10 0.0000E+00 19900101.0000 19910101.0000
GCOS1A    2    0 0.386222759789E-10 0.000000000000E+00 0.3748E-11 0.0000E+00 19500101.0000 20500101.0000
GSIN1A    2    0 0.542428904167E-10 0.000000000000E+00 0.3404E-11 0.0000E+00 19500101.0000 20500101.0000
GCOS2A    2    0 0.379017840266E-10 0.000000000000E+00 0.3617E-11 0.0000E+00 19500101.0000 20500101.0000
GSIN2A    2    0 -.163073508081E-10 0.000000000000E+00 0.3494E-11 0.0000E+00 19500101.0000 20500101.0000
```

GOCE

Gradiometre = 6 accelerometers arranged by pairs on each axis

noise ~ 3 mE.Hz$^{-1/2}$
⇔
10^{-12} m.s^{-2}.Hz$^{-1/2}$ for accelerometers 0.5 m apart

1 Eötvös = 10^{-9} s^{-2}

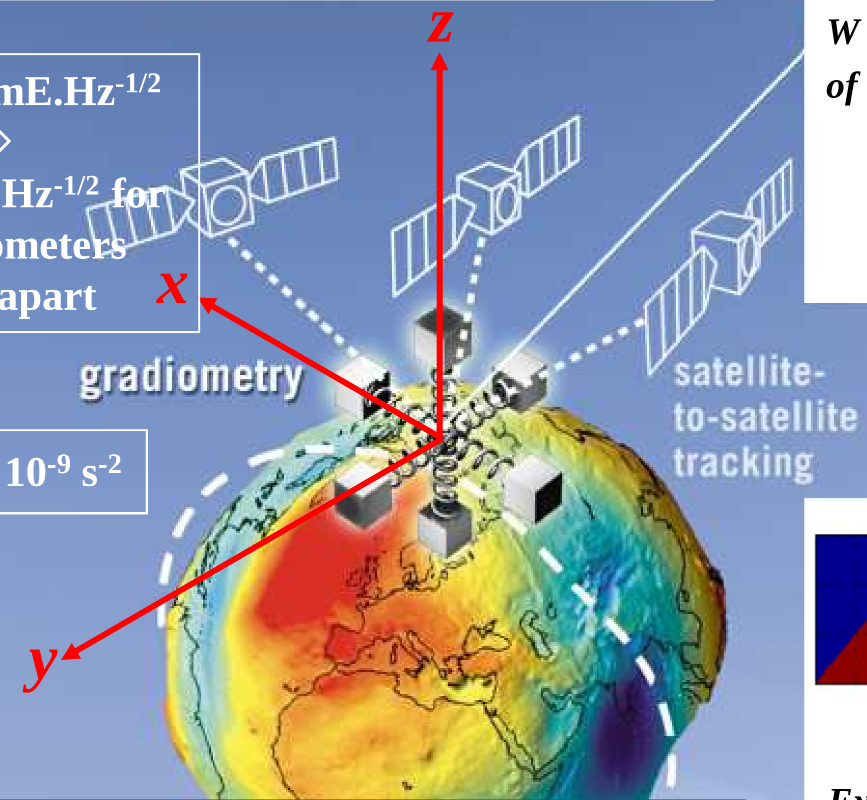

combined with GPS measurements : SST-hl

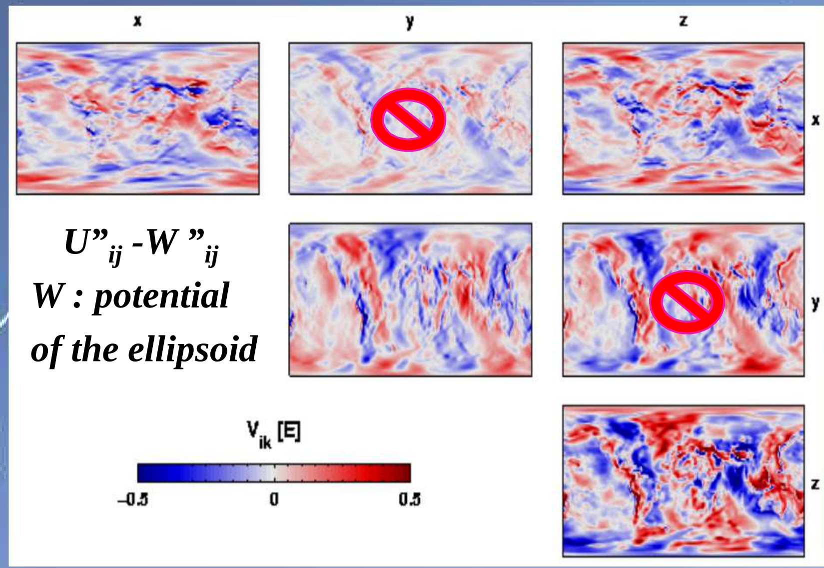

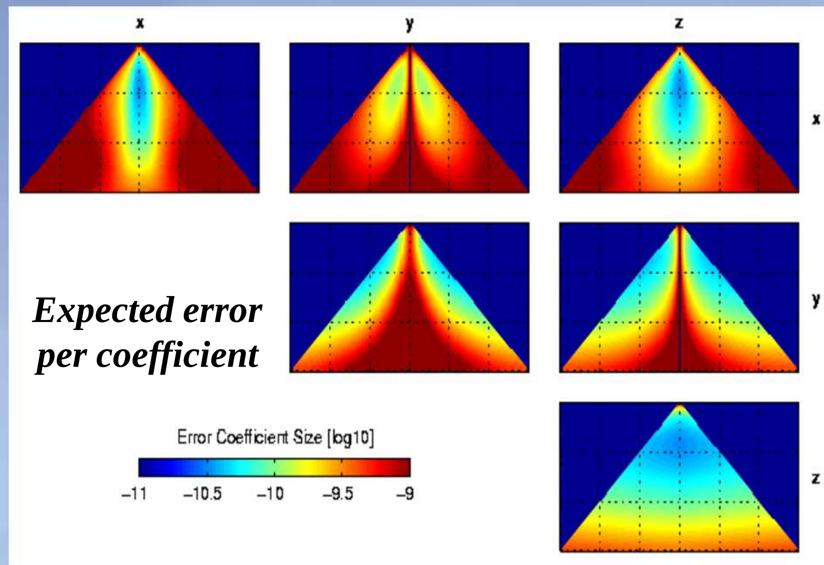

Gradiometry : *SGG*
Measure of the Gravity Gradient by Satellite

Surface data completion

Mean sea surface

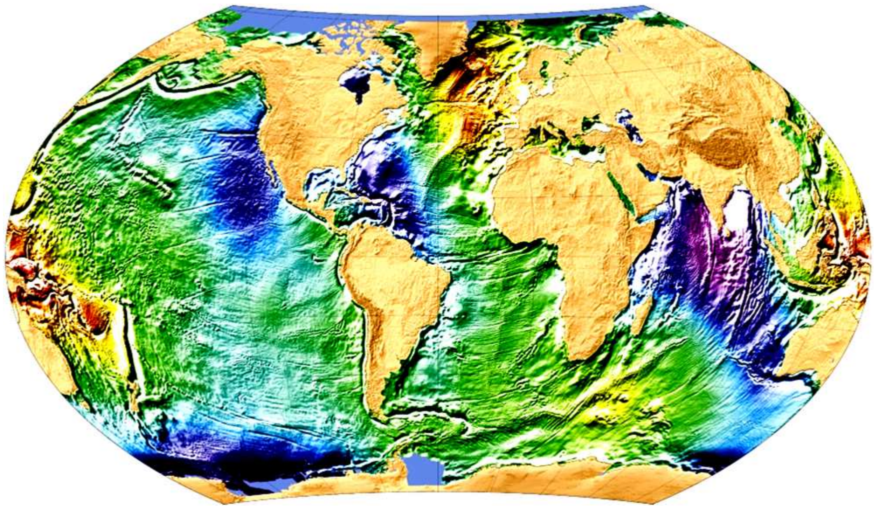

Source : CLS

Terrestrial gravimetry

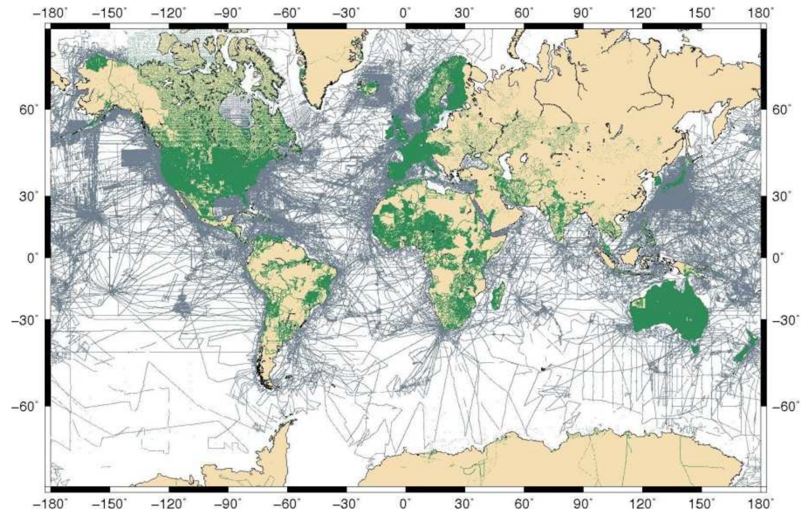

Source : BGI

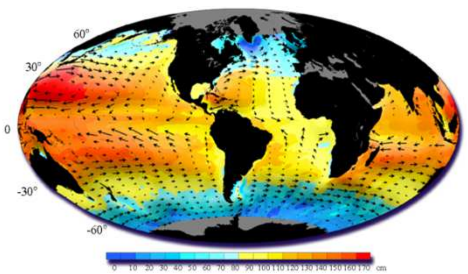

space altimetry – ocean circulation model

=> geoid height

absolute, terrain, sea gravimeters

=> gravity anomaly data

GRACE/GOCE/surface combined model: EIGEN6-C4

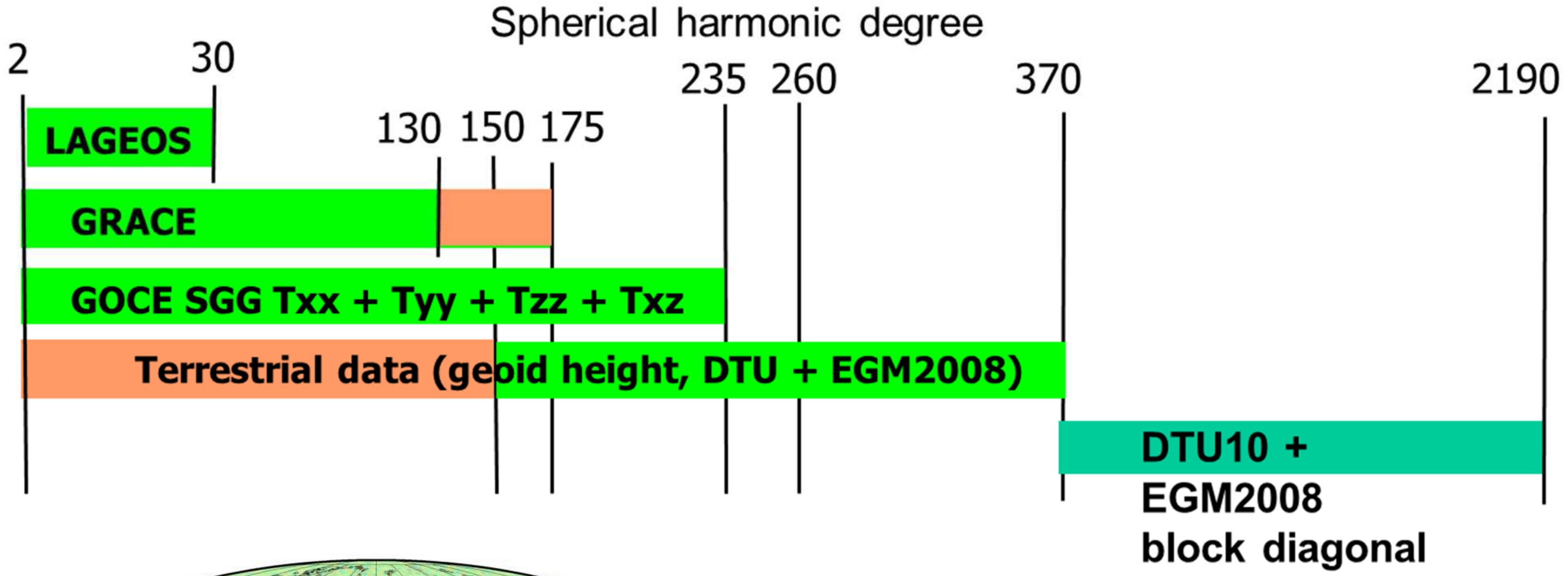

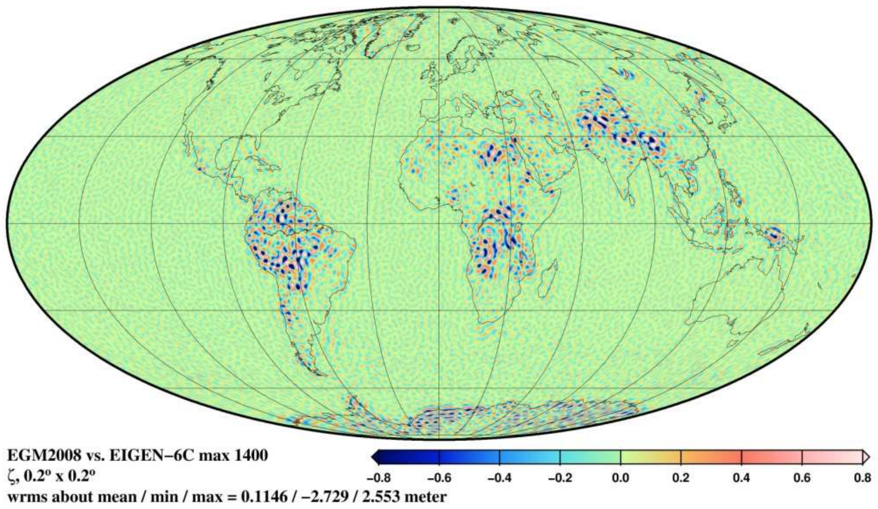

Geoid-Height Differences between:
EIGEN-6C and EGM2008

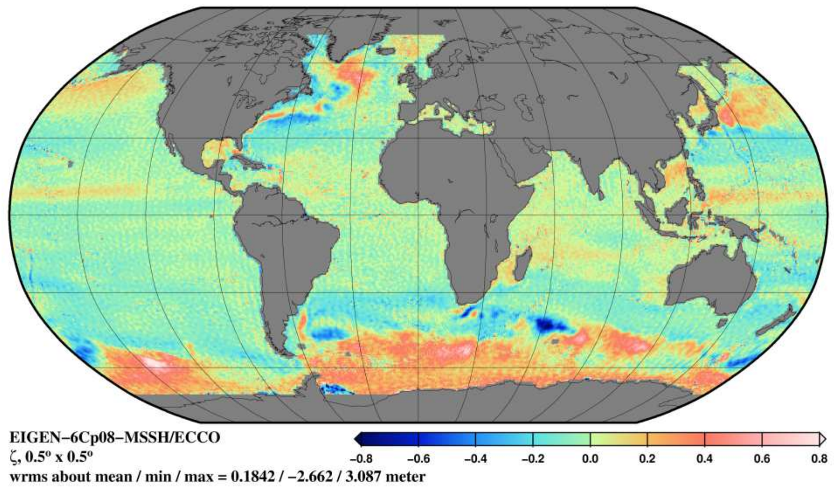

Residual Dynamic Ocean Topography (non-filtered):
EIGEN-6C – (MSSH - ECCO)

Perspective… for mapping gravity and monitoring mass transport from space

- **Satellite to satellite tracking (SST)**
  - K/Ka band measurement limited in accuracy (~µm, GRACE, GRACE-FO)
  - laser interferometer to go beyond (~nm, GRACE-FO)
  - with several satellite pairs to increase isotropy as well as spatial and temporal resolution

- **Space gradiometry**
  - electrostatic gradiometry (~10^{-12} m s^{-2} Hz$^{-1/2}$ → 3 mE Hz$^{-1/2}$, GOCE)
  - atomic gravimetry/gradiometry
  - coupled SST-atomic gradiometry systems would allow to extend the spatial spectrum from 20 000 km to a few tens of km

- **Clock**
  - clock frequency comparison along orbits (through red shift - $\Delta\nu/\nu$: 10^{-17} ⬄ ΔU: 1 m^{2}s^{-2} ⬄ Δh: 10 cm)
  - precision in orbit not yet competitive (10^{-17} on ground over a week, ACES)

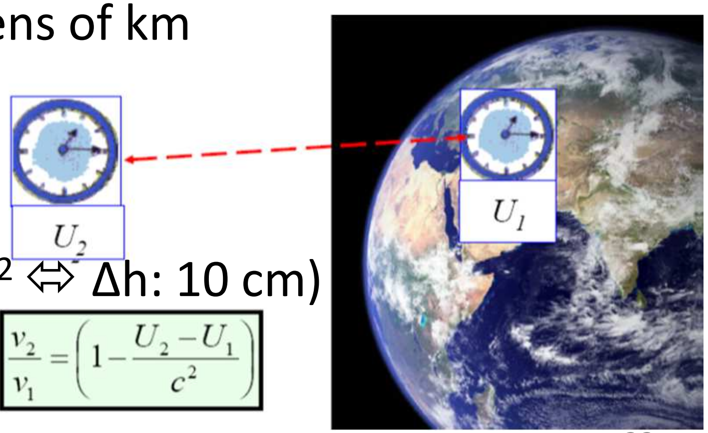

$$\frac{\nu_2}{\nu_1} = \left(1 - \frac{U_2 - U_1}{c^2}\right)$$

GRACE Follow-on (2017)

The GRACE-FO satellites are planned to be very similar to the original GRACE satellites with some improvements and a technology demonstrator for further gravity missions. The instrument consists of a frequency stabilized laser, a triple mirror assembly (retroreflector), an optical bench and an electronics board. Challenging key instrument requirements are:

- Ranging measurement accuracy of 50nm/√Hz (for 10-100 mHz)
- Laser beam co-alignment of less than 50 µrad (⇔ 10 m at 200 km)

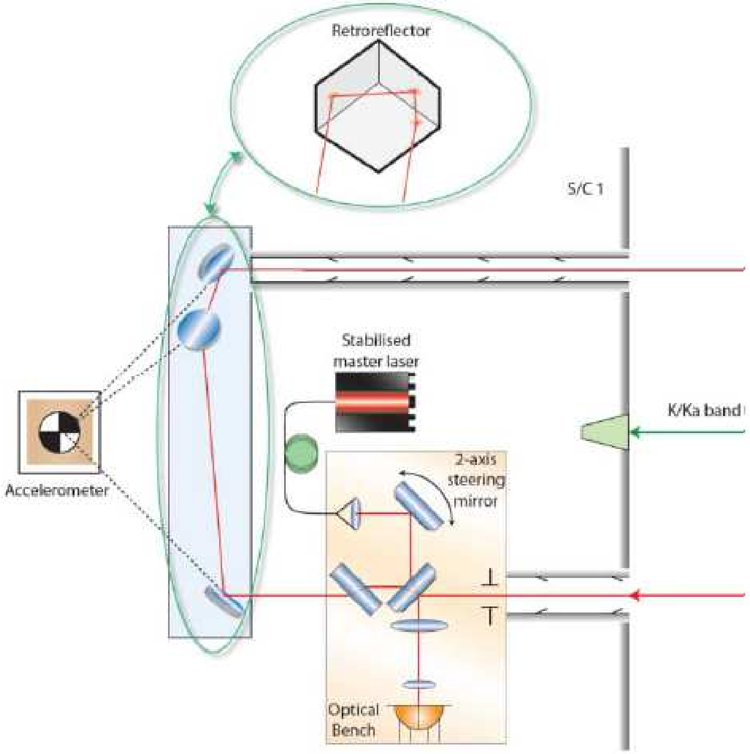

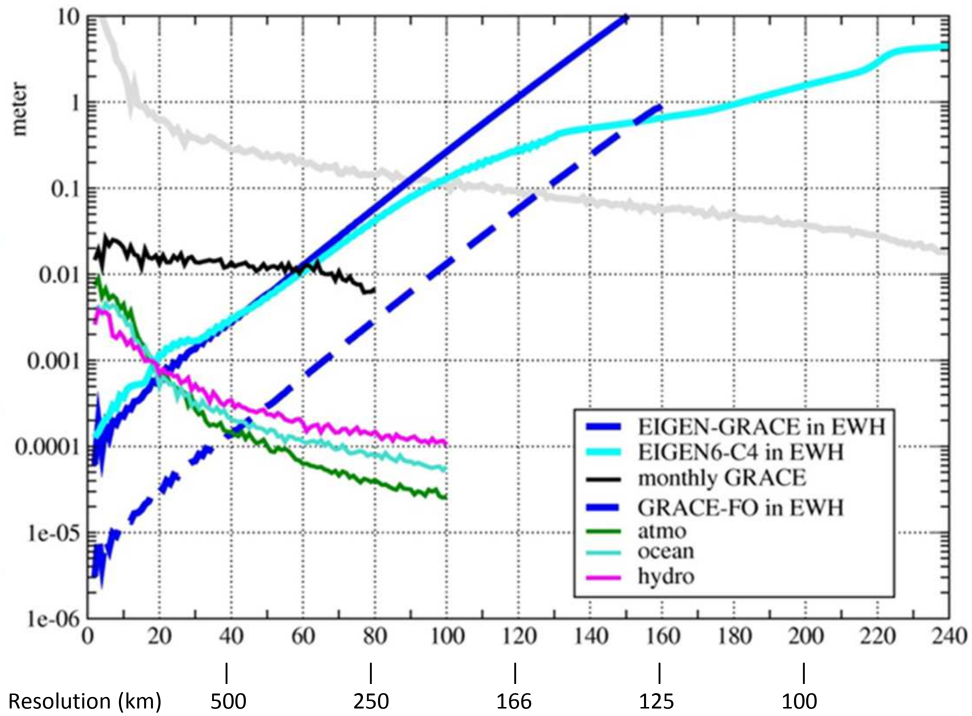

Image © Springer, from: Sheard et al. *"Intersatellite laser ranging instrument for the GRACE follow-on mission"*, Journal of Geodesy, 2012 (DOI: 10.1007/s00190-012-0566-3).

e-motion, EE-8 ESA call (2010)

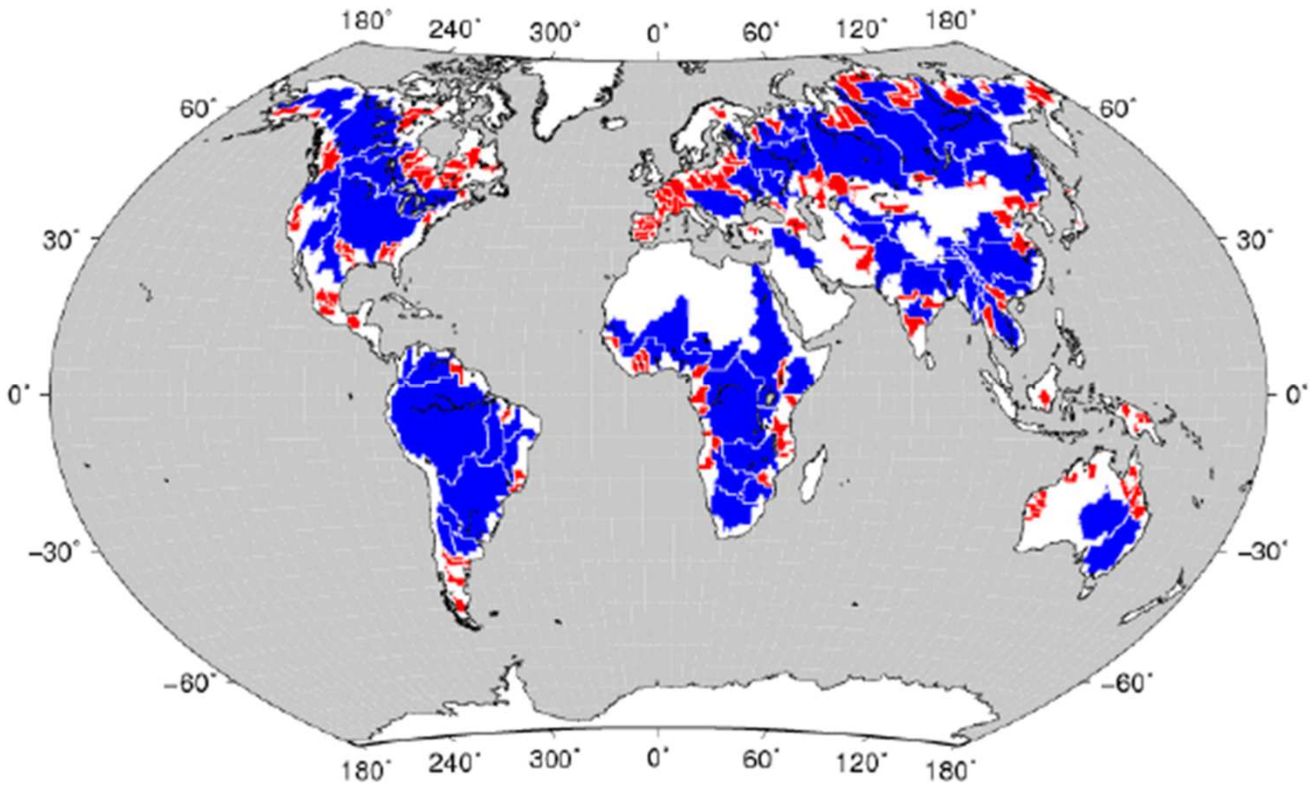

River drainage basins with a size between 40 000 km^2 and 200 000 km^2 (in red) which will be resolved by e.motion, as well as basins larger than 200 000 km^2 which corresponds to the present day resolution. e.motion will also recover sub-basin variability which plays an important role for climatic processes.

E-motion report, proposal for EE8 mission, 2010

Degree 1: geocenter

Geocenter motion from SLR

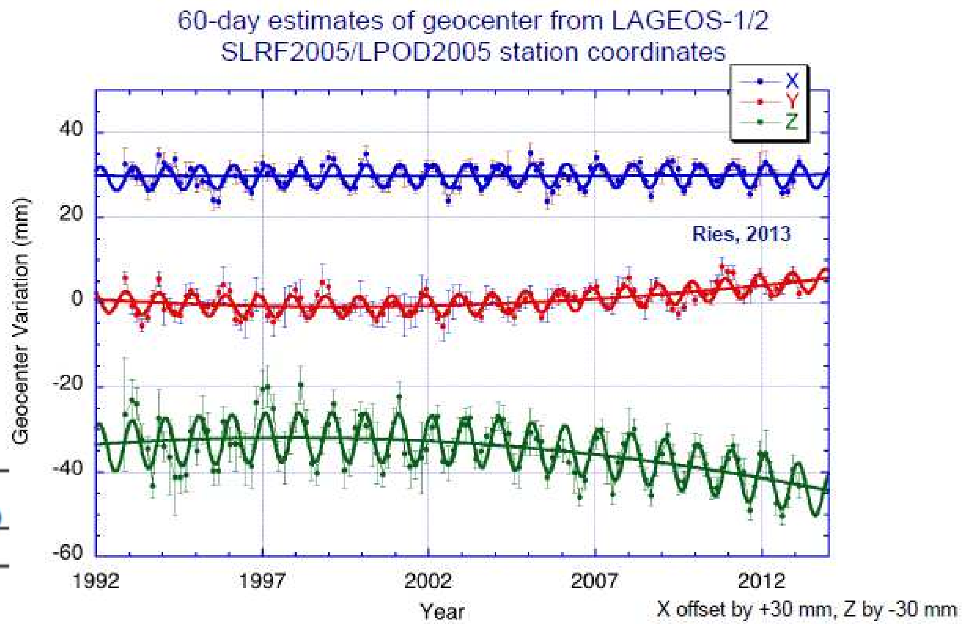

X (amp)	X (phase)	Y (amp)	Y (phase)	Z (amp)	Z (phase)	Reference (comments) (phase is in degrees)
2.8	47	2.6	324	5.8	34	Ries, 2013 (60-day estimates; 1993-2012)

Geocenter motion from geophysical models

Geophysical models of atmosphere, ocean, and hydrology can provide degree-1 mass redistribution and predict the corresponding geocenter motion after accounting for the load deformation

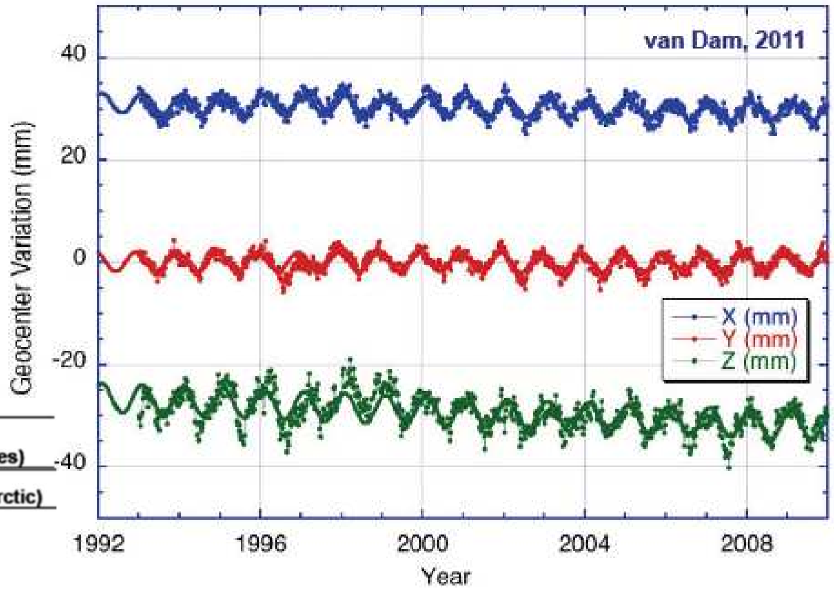

X (amp)	X (phase)	Y (amp)	Y (phase)	Z (amp)	Z (phase)	Reference (comments) (phase is in degrees)
1.9	34	1.9	337	2.8	35	van Dam, 2011 (NCEP, ECCO, GLDAS, no arctic)

Degree 2: Earth rotation and angular momentum budget

Observations:
pole motion and LOD
from *GPS, SLR, VLBI*

$$p + \frac{i}{\sigma_0}\dot{p} = \frac{k_0}{k_0 - k_2}(\chi_1 + i\chi_2) \qquad \frac{\Delta LOD}{LOD} = \chi_3$$

Euler-Liouville equations

Level of comparison

Geodetic excitation function

$$\chi = \chi^{motion} + (1 + k_2')\chi^{mass}$$

Geophysical excitation function

mass

load

GRACE + LAGEOS-1/-2 → Hydrology

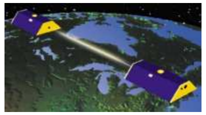

$$(\chi_1 + i\chi_2)^{mass} = -\sqrt{\frac{5}{3}}\frac{MR^2}{C - A}(\bar{C}_{21} + i\bar{S}_{21})$$

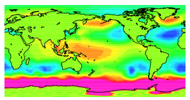

$$\chi_3^{mass} = -\frac{2\sqrt{5}}{3}\frac{MR^2}{C_m}\bar{C}_{20}$$

Atmospheric or ocean bottom pressure

Models:
meteorology,
oceanography…

Winds

$$(\chi_1 + i\chi_2)^{motion} = \frac{(h_1 + ih_2)}{\Omega(C - A)}$$

Oceanic currents

$$\chi_3^{motion} = \frac{h_3}{C_m \Omega}$$

h: angular momentum of fluid layers

Mass excitation from C21/S21

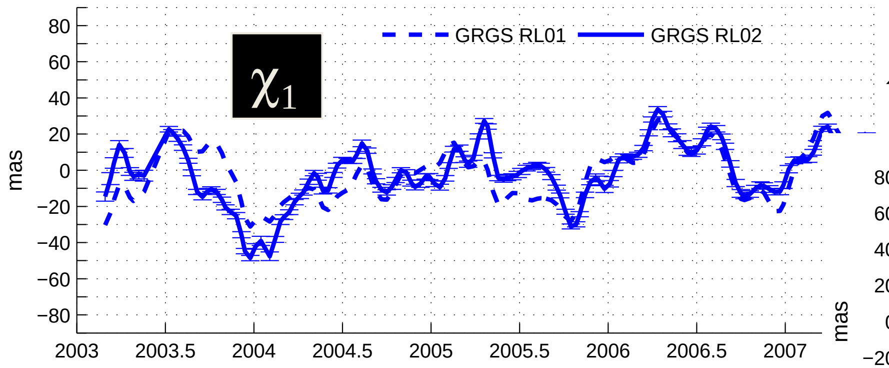

$$\chi^{mass} = \chi_1^{mass} + i\,\chi_2^{mass} = -\sqrt{\frac{5}{3}}\,\frac{MR^2}{(C-A)}(\Delta\bar{C}_{21} + i\Delta\bar{S}_{21})$$

Larger signal in RL01/02

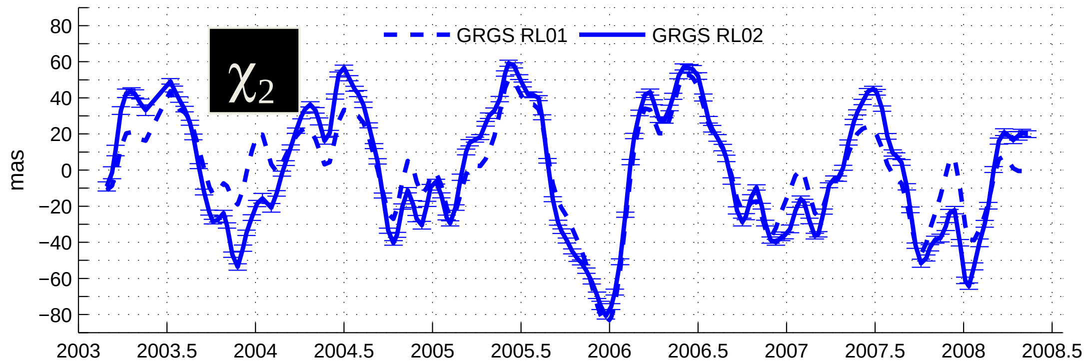

Larger signal in RL01/02

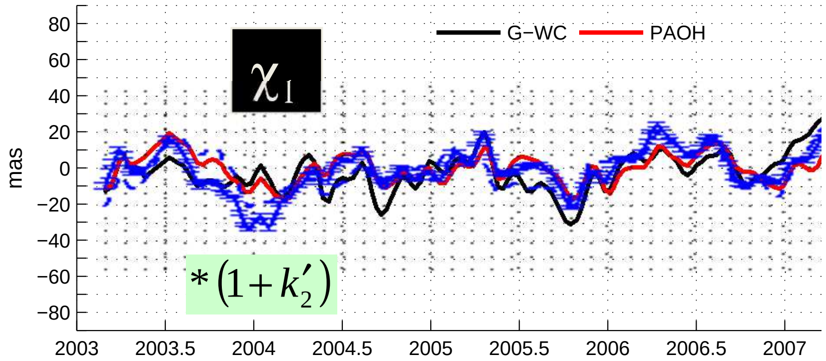

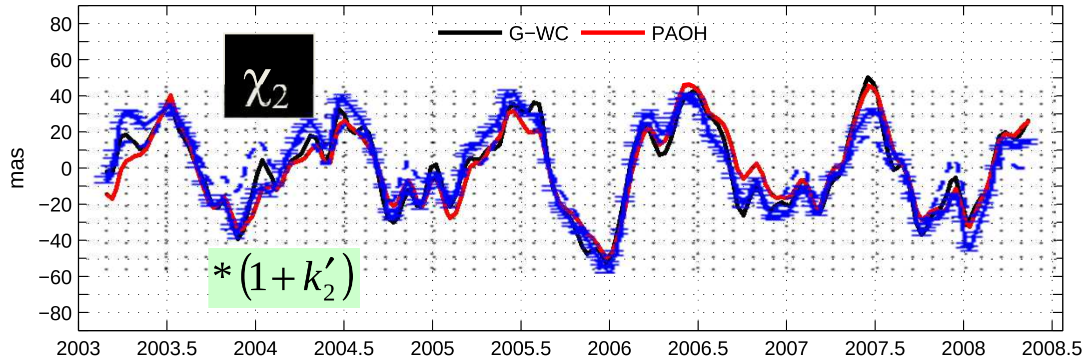

Pole rms from GPS/CO4: ~0.03 mas
⇔ ~1 mm

G-WC: geodetic excitation – motion excitation $\chi^{geodetic} - \chi^{motion}$ ⇔ ?

$(1+k_2')\,\chi^{mass}$ **RL01/02: mass excitation from GRACE/Lageos + models (ECMWF + MOG2D)**

PAOH: mass excitation from models (NCEP + ECCO + GLDAS)

Length of day (LOD) excitation

$$\chi_3^{mass} = -\frac{2\sqrt{5}}{3}\frac{MR^2}{C_m}\Delta\overline{C}_{20}$$

LOD rms from GPS/C04: ~0.008 ms ⇔ ~4 mm

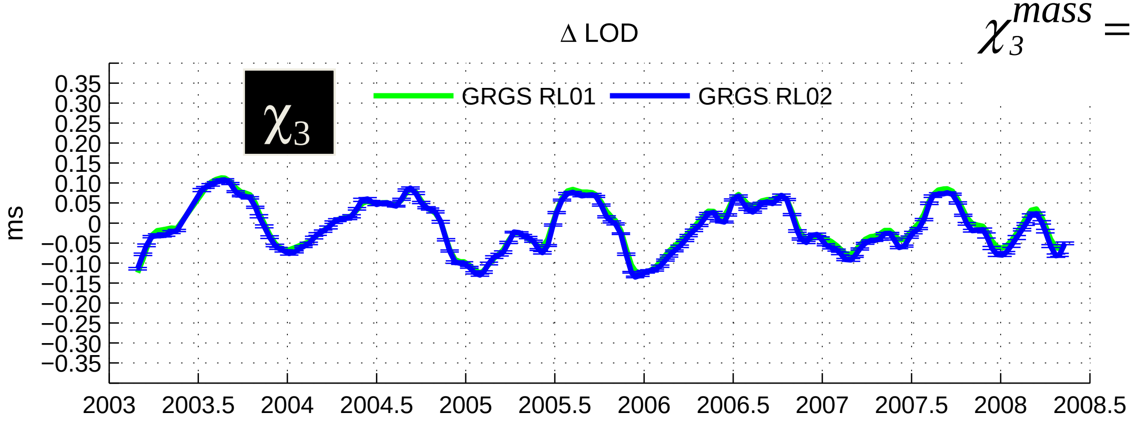

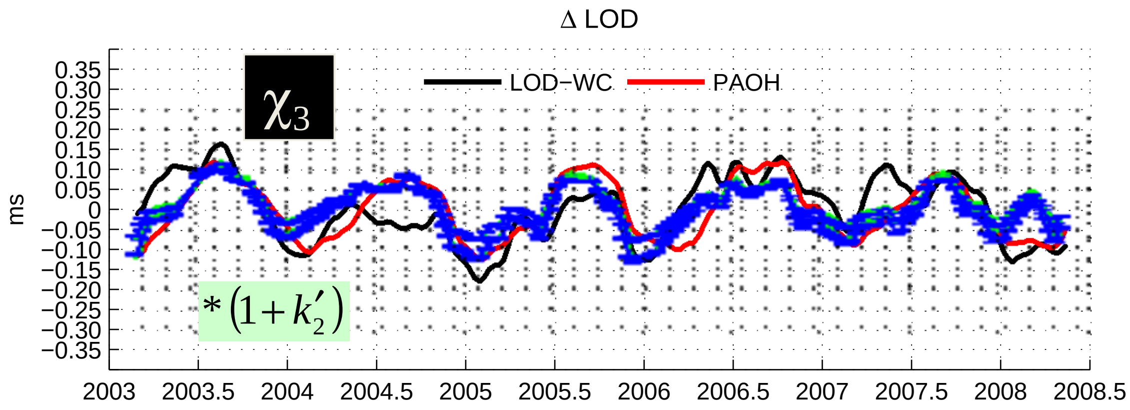

LOD-WC: geodetic excitation – motion excitation $\chi_3^{geodetic} - \chi_3^{motion}$ ⇔ **? mass excitation**

$(1+k_2')\chi_3^{mass}$ **from RL01/01: GRACE/LAGEOS + atmosphere and ocean (ECMWF+MOG2D)**

or from PAOH: NCEP + ECCO + GLDAS models

Prospective study (e-motion, 2010)

System level enhancements to improve sensitivity and isotropy :

- reducing the orbit altitude (~373 km) increases the gravity sensitivity
- tuning the inter-satellite distance impacts on wavelength of observed phenomena

Orbit configurations

- differentiating the orbit plan (normal pendulum)
- increasing the number of co-orbiting satellite pairs with different inclinations (multi-tandem: GRACE II)
- setting up relative motion formations (cartwheel)

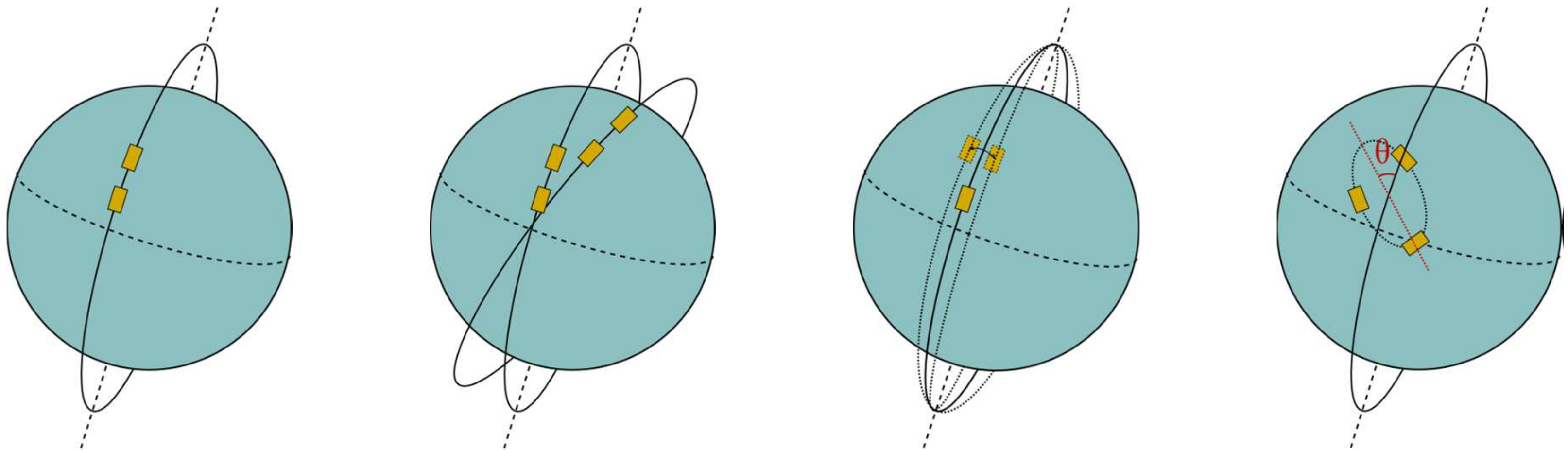

GRACE Tandem | **Double tandem** | **Normal pendulum** | **Oblique cartwheel**

Prospective study (e-motion, 2016)

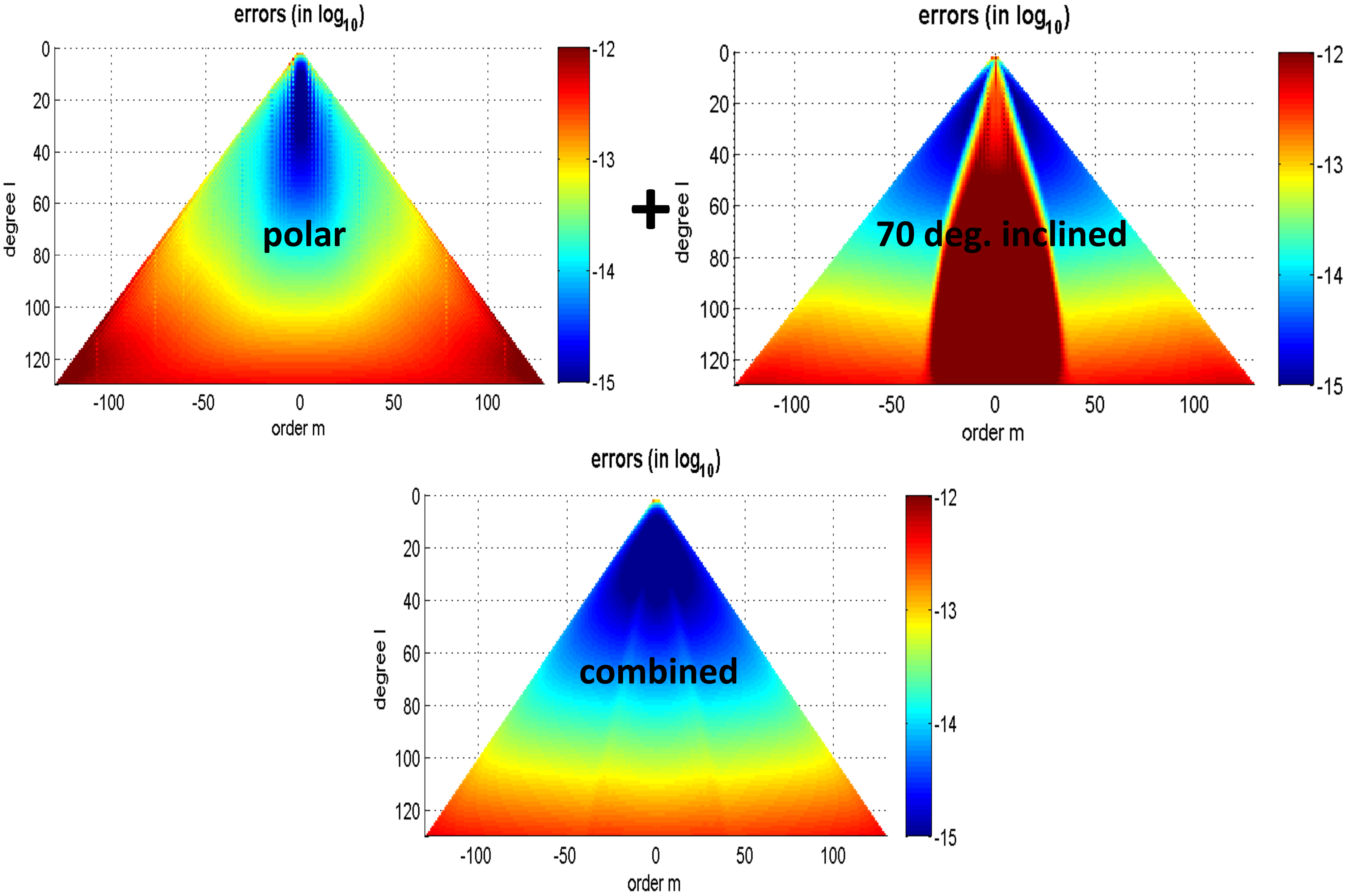

A Sharp Turn to the East

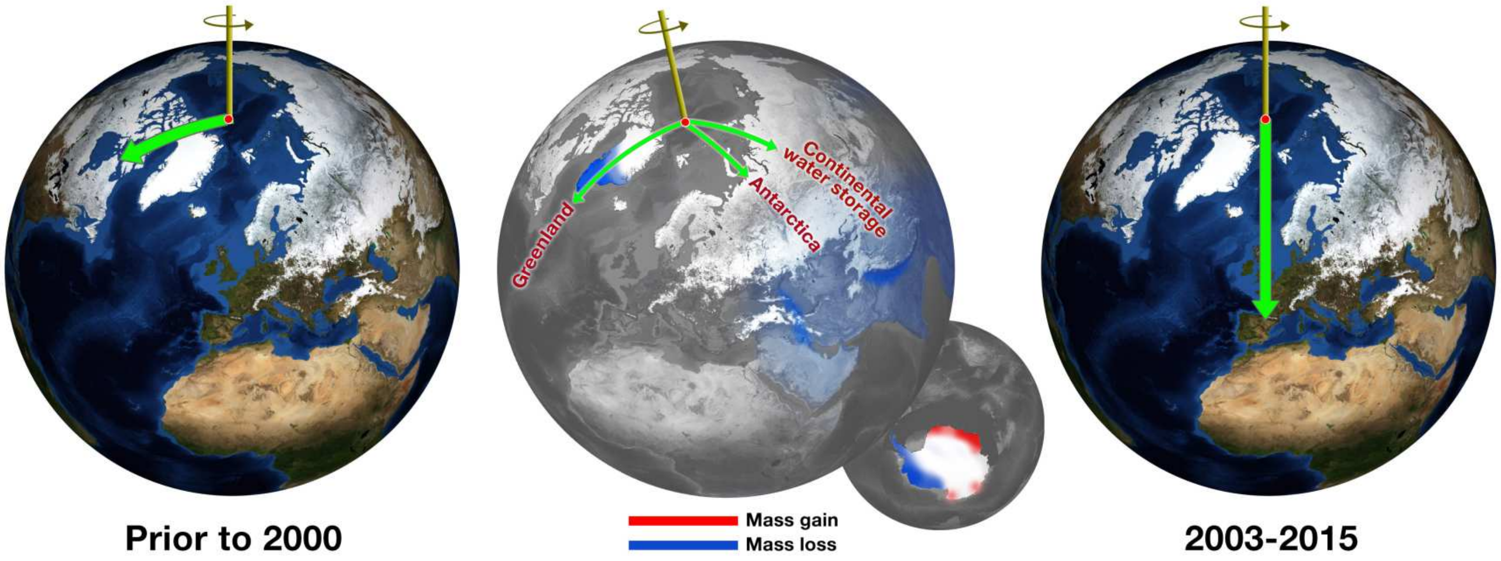

Before about 2000, Earth's spin axis was drifting toward Canada (green arrow, left globe). JPL scientists calculated the effect of changes in water mass in different regions (center globe) in pulling the direction of drift eastward and speeding the rate (right globe).

Credits: NASA/JPL-Caltech

Around the year 2000, Earth's spin axis took an abrupt turn toward the east and is now **drifting almost twice as fast as before, at a rate of almost 17 centimeters a year**. Scientists have suggested that the **loss of mass from Greenland and Antarctica's rapidly melting ice sheet** could be causing the eastward shift of the spin axis.

Ice mass loss from GRACE

post-glacial rebound (GIA)

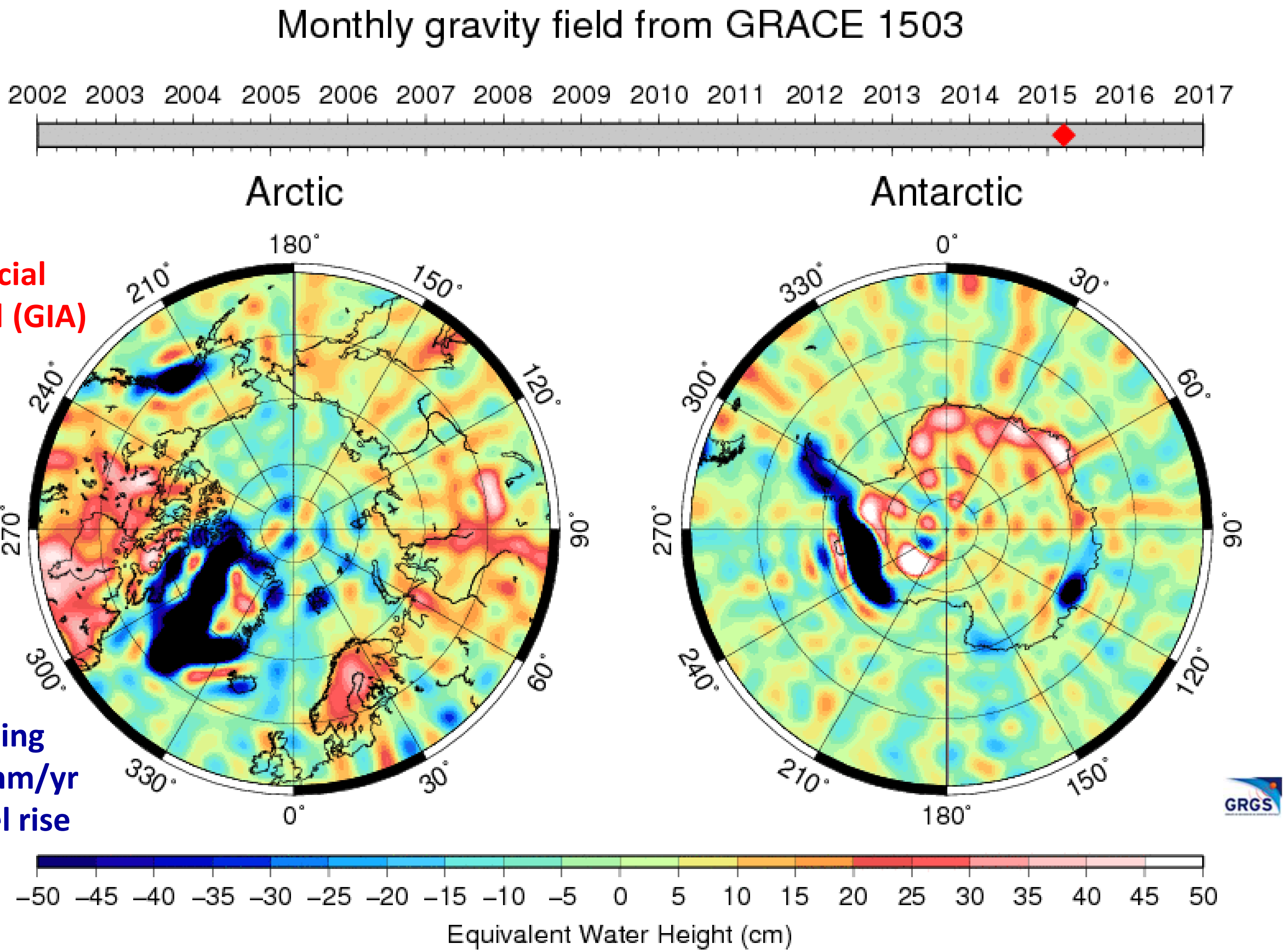

ice melting
→ 1.8 mm/yr
sea level rise

http://grgs.obs-mip.fr/grace

Altitude of the oceans from altimetry and GOCE

In geostrophic conditions:

$$\text{Eastward velocity: } \dot{x}(\varphi,\lambda) = -\frac{g}{2\Omega \sin\varphi\, R}\frac{\partial h(\varphi,\lambda)}{\partial\varphi}$$

$$\text{Northward velocity: } \dot{y}(\varphi,\lambda) = -\frac{g}{2\Omega \sin\varphi\, R\cos\varphi}\frac{\partial h(\varphi,\lambda)}{\partial\lambda}$$

h: mean dynamic topography = mean sea surface – geoid

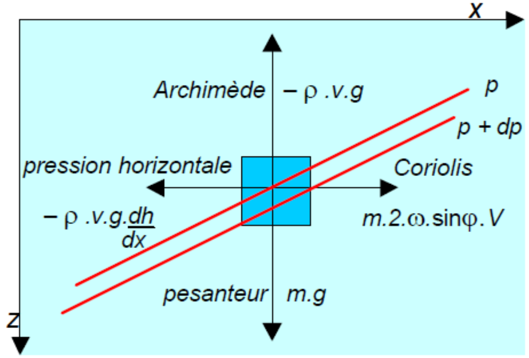

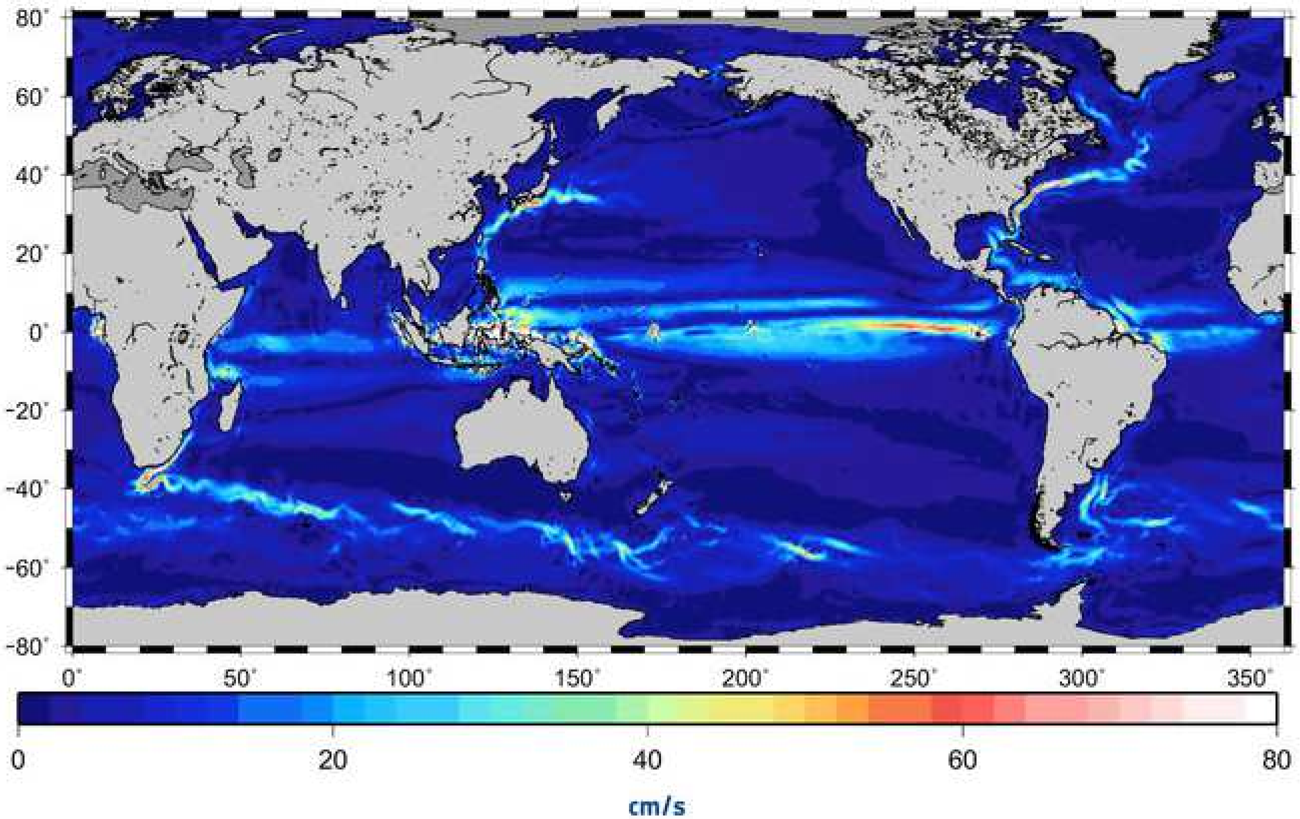

-1.6m < h < 1.6m

CLS

Geostrophic currents derived from altimetry and GOCE

The relative accuracy of the geoid models was assessed through the comparison of the mean geostrophic currents: Mean Dynamic Topographies (MDT; mean sea surface minus geoid) are computed and filtered at **spatial scales ranging from 80-200 km** with a Gaussian filter, then associated mean geostrophic currents are compared to mean geostrophic currents derived from **independent drifting buoy data**, available in all oceans, and similarly filtered. The standard deviation of the difference is then calculated. The surface velocities are inferred with an **uncertainty of 3 cm/s from drifter trajectories**, after the ageostrophic components and the time variability measured by altimeters have been removed.

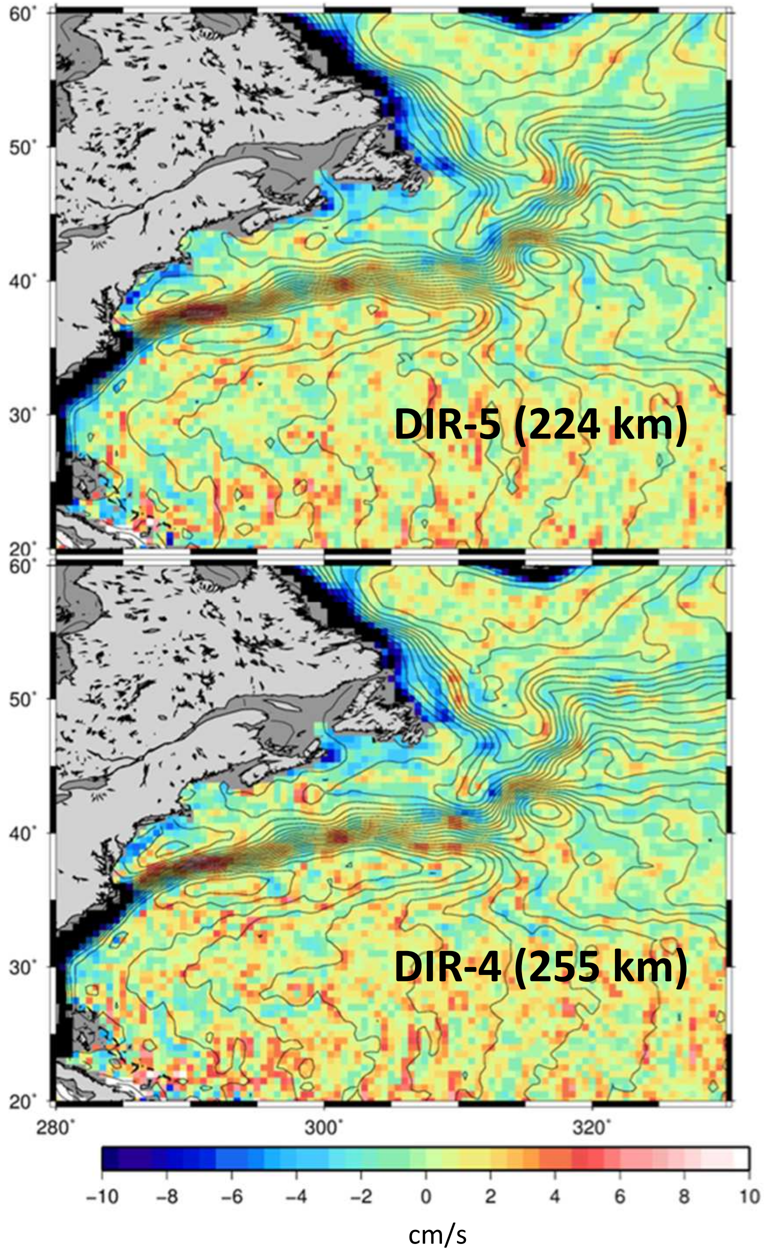

Differences with drifter current intensities for DIR-R5 (top) and DIR-R4 (bottom) for the Gulf Stream. The MDT contour lines are superposed.

Altimetric validation

❖ **The new RL03-v2 model** reduces the **geographically correlated radial orbit drift rate**, from more than 1 mm/yr (for the RL02bis mean model) to less than 0.6 mm/yr over ~7 years, with respect to Jason-2 GDR-E reduced-dynamic orbits (from GPS+DORIS).

❖ Jason-2 SLR residuals :

➢ RL02: 1.36 cm rms

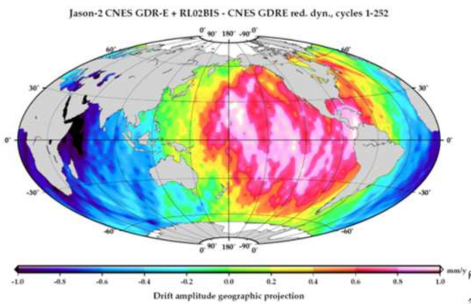

Radial orbit drift rate
Scale: -1 / +1 mm/yr
[A. Couhert & al., 2015]

➢ RL03-v2: 1.29 cm rms

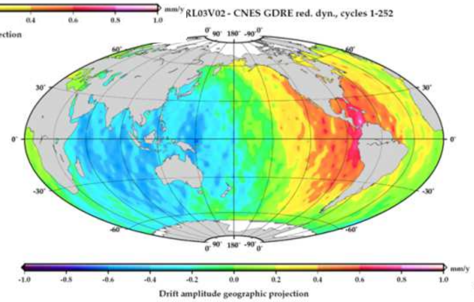

➢ RL03-v2 + C31 adjusted: 1.27 cm rms

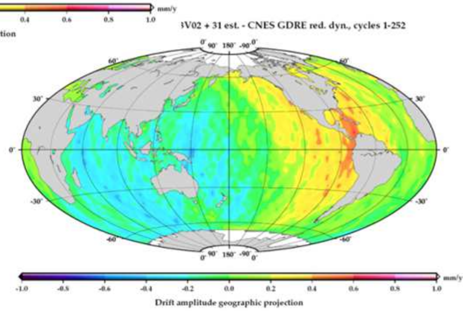

More information